Tran-SET

Transportation Consortium of South-Central States

Solving Emerging Transportation Resiliency, Sustainability, and Economic Challenges through the Use of Innovative Materials and Construction Methods: From Research to Implementation

Residual Life and Reliability Assessment of Underground RC Sanitary Sewer Pipelines under Uncertainty

Project No. 20STUTA25

Lead University: University of Texas at Arlington

Final Report

August 2021

Disclaimer

The contents of this report reflect the views of the authors, who are responsible for the facts and the accuracy of the information presented herein. This document is disseminated in the interest of information exchange. The report is funded, partially or entirely, by a grant from the U.S. Department of Transportation's University Transportation Centers Program. However, the U.S. Government assumes no liability for the contents or use thereof.

TECHNICAL DOCUMENTATION PAGE

1. Project No.	2. Government Accession No.	3. Recipient's Catalog No.
20STUTA25		

4. Title and Subtitle	5. Report Date
Residual Life and Reliability Assessment of Underground RC sanitary Sewer Pipelines Under Uncertainty	Aug. 2021
	6. Performing Organization Code
7. Author(s)	**8. Performing Organization Report No.**
PI: Himan Hojat Jalali https://orcid.org/0000-0002-0075-9725 GRA: Moein Ebrahimi https://orcid.org/0000-0003-3602-2423	
9. Performing Organization Name and Address	**10. Work Unit No. (TRAIS)**
Transportation Consortium of South-Central States (Tran-SET) University Transportation Center for Region 6 3319 Patrick F. Taylor Hall, Louisiana State University, Baton Rouge, LA 70803	**11. Contract or Grant No.** 69A3551747106
12. Sponsoring Agency Name and Address	**13. Type of Report and Period Covered**
United States of America Department of Transportation Research and Innovative Technology Administration	Final Research Report August 2020 –August 2021
	14. Sponsoring Agency Code

15. Supplementary Notes

Report uploaded and accessible at Tran-SET's website (http://transet.lsu.edu/).

16. Abstract

Prioritization of limited funding for pipelines maintenance is a major issue that concerns municipalities nationwide. Conducting a probabilistic assessment can provide a complete characterization of the performance of structural elements and systems along with optimizing the limited resources. The most widely used probabilistic performance indicator is reliability, a measure of the probability of failure corresponding to a particular limit state (e.g., ultimate strength or serviceability). Reliability methods can be used to identify which pipeline sections within a particular system require the most urgent inspection or repair. To this end, an automated data-driven framework for large diameter reinforced concrete pipes (RCPs) is developed that converts the raw unfiltered inspection readings to data that is used for estimating residual life and further reliability assessment purposes. In the current work, initially, the wall thickness erosion is determined based on the inspection data collected using Light Detection and Ranging (LiDAR). Furthermore, the best fit among several probability distribution functions for the wall thickness loss is obtained, which is integrated with a serviceability limit state that defines failure as the complete loss of 1-in concrete cover caused by environmental conditions such as sulfide-induced erosion. Considering this limit state and a prescribed probability of exceedance threshold, a reliability-based prediction of the remaining service life is proposed. The developed framework requires minimal user interference and is, therefore, less time consuming and more consistent compared to previous research. From an asset management point of view, the most vulnerable pipeline sections are identified that will require further inspection and attention. This will provide decision makers crucial information regarding the current state of the pipeline network, to better allocate the already scarce maintenance funding of these pipelines.

17. Key Words	18. Distribution Statement
Remaining service life, Reinforced concrete, Sanitary sewer, Data-driven approach	No restrictions. This document is available through the National Technical Information Service, Springfield, VA 22161.

19. Security Classif. (of this report)	20. Security Classif. (of this page)	21. No. of Pages	22. Price
Unclassified	Unclassified	59	

Form DOT F 1700.7 (8-72) **Reproduction of completed page authorized.**

SI* (MODERN METRIC) CONVERSION FACTORS

APPROXIMATE CONVERSIONS TO SI UNITS

Symbol	When You Know	Multiply By	To Find	Symbol
		LENGTH		
in	inches	25.4	millimeters	mm
ft	feet	0.305	meters	m
yd	yards	0.914	meters	m
mi	miles	1.61	kilometers	km
		AREA		
in^2	square inches	645.2	square millimeters	mm^2
ft^2	square feet	0.093	square meters	m^2
yd^2	square yard	0.836	square meters	m^2
ac	acres	0.405	hectares	ha
mi^2	square miles	2.59	square kilometers	km^2
		VOLUME		
fl oz	fluid ounces	29.57	milliliters	mL
gal	gallons	3.785	liters	L
ft^3	cubic feet	0.028	cubic meters	m^3
yd^3	cubic yards	0.765	cubic meters	m^3
		NOTE: volumes greater than 1000 L shall be shown in m^3		
		MASS		
oz	ounces	28.35	grams	g
lb	pounds	0.454	kilograms	kg
T	short tons (2000 lb)	0.907	megagrams (or "metric ton")	Mg (or "t")
		TEMPERATURE (exact degrees)		
^oF	Fahrenheit	5 (F-32)/9 or (F-32)/1.8	Celsius	^oC
		ILLUMINATION		
fc	foot-candles	10.76	lux	lx
fl	foot-Lamberts	3.426	candela/m^2	cd/m^2
		FORCE and PRESSURE or STRESS		
lbf	poundforce	4.45	newtons	N
lbf/in^2	poundforce per square inch	6.89	kilopascals	kPa

APPROXIMATE CONVERSIONS FROM SI UNITS

Symbol	When You Know	Multiply By	To Find	Symbol
		LENGTH		
mm	millimeters	0.039	inches	in
m	meters	3.28	feet	ft
m	meters	1.09	yards	yd
km	kilometers	0.621	miles	mi
		AREA		
mm^2	square millimeters	0.0016	square inches	in^2
m^2	square meters	10.764	square feet	ft^2
m^2	square meters	1.195	square yards	yd^2
ha	hectares	2.47	acres	ac
km^2	square kilometers	0.386	square miles	mi^2
		VOLUME		
mL	milliliters	0.034	fluid ounces	fl oz
L	liters	0.264	gallons	gal
m^3	cubic meters	35.314	cubic feet	ft^3
m^3	cubic meters	1.307	cubic yards	yd^3
		MASS		
g	grams	0.035	ounces	oz
kg	kilograms	2.202	pounds	lb
Mg (or "t")	megagrams (or "metric ton")	1.103	short tons (2000 lb)	T
		TEMPERATURE (exact degrees)		
^oC	Celsius	1.8C+32	Fahrenheit	^oF
		ILLUMINATION		
lx	lux	0.0929	foot-candles	fc
cd/m^2	candela/m^2	0.2919	foot-Lamberts	fl
		FORCE and PRESSURE or STRESS		
N	newtons	0.225	poundforce	lbf
kPa	kilopascals	0.145	poundforce per square inch	lbf/in^2

TABLE OF CONTENTS

LIST OF FIGURES

LIST OF TABLES

ACRONYMS, ABBREVIATIONS, AND SYMBOLS

ASTM	American Section of the International Association for Testing Materials
CCTV	Closed-Circuit Television
CIPP	Cast in Place Pipe
LiDAR	Light Detection and Ranging
LS	Least Squares
M-M	Manhole to Manhole
MSI	Multi-Sensor Inspection
PDF	Probability Distribution Function
RCP	Reinforce Concrete Pipeline
Tran-SET	Transportation Consortium of South-Central States

EXECUTIVE SUMMARY

The objective of this project is to determine the residual service life of reinforced concrete (RC) sanitary pipeline using a reliability-based method. The most conventional method for pipeline inspection is closed-circuit television (CCTV) due to its cost effectiveness; however, CCTV inspection is not capable of calculating the degradation of inner wall thickness of RC pipelines caused by sulfide corrosion, which is necessary for estimating the residual service life of sewer RCPs for asset management purposes. The data is often collected using laser or Light Detection and Ranging (LiDAR) technology. The LiDAR typically used for these inspections has an accuracy of ± 1 mm. Therefore, it is a great technology for calculating the inner wall thickness loss of sanitary sewer pipelines for residual service life estimation.

In current work, an automated data driven framework with minimal user interference is developed that uses LiDAR data from sewer inspections (provided by Redzone Robotics and the Center for Structural Engineering Research/Simulation and Pipeline Inspection (CSER/SPI)) to obtain necessary information for estimation of pipe-wall thickness loss in sanitary sewer lines. The LiDAR point cloud of data, collected for each 5-ft. length of a pipeline (M-M), contains noises such as water level points and pipeline defects (e.g., root intrusion). After filtering and alignment of data cloud, each 5-ft section of the pipeline is divided into 60 rings, each having a length of 1-in. This allows to determine the wall thickness loss for each ring with greater accuracy.

Once the pipe wall thickness loss is estimated using the filtered LiDAR data, corrosion rate is calculated by dividing the wall thickness loss amount to the age of the pipeline. Furthermore, a best distribution is fitted to wall thickness loss data. The goodness of fit is calculated by comparing R^2 values from least squares (LS) for QQ-plots of 11 different distribution. Finally, reliability is calculated considering serviceability limit state that defines failure as the complete loss of 1-in concrete cover. Considering this limit state and a prescribed probability of exceedance threshold, a reliability-based prediction of the remaining service life is determined for 1000 linear foot of large diameter RC sewer lines inspected by Redzone Robotics and CSER/SPI at University of Texas at Arlington with diameters of 54 and 60 inches. The result of the proposed approach is consistent, and reasonable with minimum user interference. To have a better vision on pipeline assessment, the results are provided for each 5-ft section of each sewer line (M-M). The anticipated results can assist decision makers in prioritizing limited repair funding by providing a comprehensive, network-level, quantitative performance assessment of selected RC sanitary pipelines using the proposed automated framework.

1. INTRODUCTION

Sewer pipelines are an important part of the infrastructure that carry the wastewater out of cities. The Romans, Persians, Athenians, Macedonians, and Greeks built the early versions of sewer systems from stone and cement. Sewer systems comprise about fifty percent of the underground infrastructure in the United States *(1)*, which includes more than 1,300,000 miles of public and private sewer lines. The serviceability of these sewer lines can be affected by structural failure, overflows, and blockages. In 2017, American Society of Civil Engineers (ASCE) ranked this infrastructure as a D+ *(2)*, and anticipated over 56 million people will be connected to the centralized treatment plants by 2032. The biggest challenge for municipalities and decision makers is maintenance of infrastructures in their inventory and prioritizing limited repair funding. Sanitary sewer mains are the most vital underground infrastructure, and they play a major role in having a sustainable urban system. Due to the importance of these underground infrastructure, the sewer systems are expected to have a longer service life than typical civil engineering structures. Thus, it is crucial to provide an acceptable level of infrastructures serviceability and to make a balance between the maintenance costs and risk of failures.

Available methods for monitoring the sewer conditions, such as visual inspection by CCTV, LiDAR, laser profiling, or sonar can be used independently or combined to monitor sewer lines *(3)*. CCTV monitoring is a well-established inspection method among municipalities due to its cost-effectiveness and simplicity as compared to other methods of sewer line inspection However, this method is subjective if it is used as the sole inspection method, since it depends solely on the opinion of the trained personnel monitoring the CCTV feeds. As a result, employing another inspection technique in conjunction with CCTV is helpful to reduce subjectivity and errors *(4)*. Since sewer pipes often fail abruptly without prior warning, it is necessary to properly plan for the inspection cycles for decreasing the failure rates.

In this study, the residual service life of large RC sanitary sewer pipelines with diameters of 54” and 60” is estimated based on probabilistic and reliability-based automated data-driven framework by incorporating inspection data for 10,000 linear foot of sewer lines. To this end, the critical input information is the current erosion of pipe cross-sections, which is obtained through the inspection data in the form of LiDAR measurements. The proposed automated framework is developed to get the LiDAR raw output data and apply filtering, aligning, and to obtain the cross-section wall thickness loss. Furthermore, different probability distribution functions are fitted to the wall thickness loss data and a best fit is obtained. Moreover, based on the corrosion rate and a selected confidence level, the reliability-based residual life of the inspected lines are provided. Based on the decision makers’ resources, the results could be presented at different scales, whether for small 1-inch rings, 5-foot sections, or even for the whole inspected line (M-M).

2. OBJECTIVES

The overall objective of this study is to develop an innovative, automated and rational framework for condition assessment RC sanitary sewer pipelines as part of the transportation infrastructure in Region 6.

More specifically the objectives of the research are to:

- Find the best probability density function (PDF) for representing the concrete wall-thickness loss due to sulfide-induced erosion.
- Estimate the residual service life of RC sewer pipes using the wall-thickness loss serviceability limit state function, one of the most common structural deteriorations in RCPs based on field inspection of sewer lines using LiDAR technology. Also, compare the life expectancy of sewer pipes considering different PDFs for wall-thickness losses.
- Develop an automated framework with minimum user interference to enhance consistency and reliability. The algorithm can process the point cloud of data (i.e., the output of the LiDAR inspection) and provide a reliability-based life assessment of each pipeline. It also seeks to provide a more simplistic criteria (i.e., the standard deviation of loss data) to find the most critical section of RC pipeline.

3. LITERATURE REVIEW

The most challenging task in developing a life-cycle management for sanitary sewer systems is the maintenance of the aging infrastructure. In the sewer pipes inventory, many of these pipes are reaching the end of their service life and as a result municipality are looking for methods for condition assessment with the goal to estimate their residual service life. In the following section, mechanism of deterioration of RC pipe is discussed; the main factor behind this deterioration is explained. The multi-sensor inspection (MSI) technologies are explained. Furthermore, probabilistic methods to model the deterioration of RC pipes due to corrosion is explained.

3.1. Deterioration mechanism of Sanitary Sewer Pipeline

RC sanitary sewer pipes are susceptible to different types of deterioration that threaten their structural capacity and serviceability. Failure of these structures, or losing parts of their operational capabilities, may cause undesirable consequences that affect the surrounding environment, public health, and the economy. In some cases, the sewer pipe collapse could be lethal: e.g. a deputy was killed in West Side Road in San Antonio in 2016 *(5)*. Some of the most important sewer pipe damages are crack, corrosion, roots intrusion, breakage, and misaligned connection. Among these, crack, corrosion, and breakage can result in more than half of the collapses in sewer systems *(6)*. A common damage observed in RCPs is the corrosion due to the existence of hydrogen sulfide (H_2S). This process is as follows:

1. Newly cast concrete has high alkalinity (the pH of 12-13) which is the result of formation of $CaOH_2$. This hinders the formation of microorganism *(7)*. This stage is called Abiotic Neutralization. In the meantime, the sulfate reducing bacteria (SRB) exist in the biofilm along the perimeter of the submerged surface. SRB converts the sulfate (SO_4^{-2}) into hydrogen sulfide and oxidized to form carbon dioxide (CO_2).

$$\text{Organic matter} + SO_4^{-2} \longrightarrow H_2S + CO_2 \qquad [1]$$

Some aspects such as low flow velocities, long sewage flows, and high sewage temperatures accelerate the formation of H_2S. H_2S gas and CO_2 dissolve in a biofilm to form HS^- and H^+ and a weak bicarbonate acid (H_2CO_3); then, this reacts with the alkali species in concrete (calcium hydroxide) to decrease pH down to 9. The estimated period for this process is few months and could extended to few years *(8)*.

2. Creating of neutrophilic bacteria (sulfur reducing bacteria NOSM): when the pH drops to 9 and due to sufficient presence of nutrient and oxygen, sulfur reducing bacteria (Thiobacillus) initiate to colonize on the concrete surface. As NOSM grows, the oxidation of the sulfur ions (S^{-2}) is facilitated in the sulfuric acid to form hydrogen sulfate acid (H_2SO_4). This acid will further react with concrete surface to drop the pH more. This step is called Biotic corrosion *(9)*.

$$H_2S + 2O_2 \xrightarrow{\text{NOSM}} H_2SO_4 \qquad [2]$$

3. Colonization by Acidophilic bacteria (ASOM): ASOM start to grow once the pH drops to 4, it has the same role as NOSM *(10)*; it oxidizes the elemental sulfur and the thiosulfate ($S_2O_3^{-2}$). This process will further drop the pH to 1-2.

4. Initiation of loss of cover: The H_2SO_4 which results from the oxidation of the H_2S (by the ASOM) reacts with carbonate and silicate products in concrete mix to make calcium sulfate $CaSO_4$ (gypsum). The effect of biological H_2S corrosion in RCP is bigger when the concrete contains limestone aggregate. Gypsum accumulates on the perimeter of the unsubmerged surface.

$$H_2SO_4+CaO.SiO_2.2H_2O \longrightarrow CaSO_4+SI(OH)_4+H_2O \quad [3]$$

$$H_2SO_4+CaCO_3 \longrightarrow CaSO_4+H_2CO_3 \quad [4]$$

$$H_2SO_4+Ca(OH)_2 \longrightarrow CaSO_4+2H_2O \quad [5]$$

Gypsum will further react with the tricalcium aluminate to form ettringite ($3CaO.Al_2O_3.3CaSO_4.31H_2O$).

$$CaSO_4+3CaO.AL_2O_3.6H_2O+25H_2 \longrightarrow 3CaO.AL_2O_3.3CaSO_4.31H_2O \quad [6]$$

This chemical process is outlined in Figure 1. In general, the corrosion in concrete sewer pipes happens quickly (usually 3 to 6 months) with the constant presence of hydrogen sulfide in the sewer environment. A more detailed literature review on the mechanism of sulfide-induced erosion can be found in Abuhishmeh *(11)*.

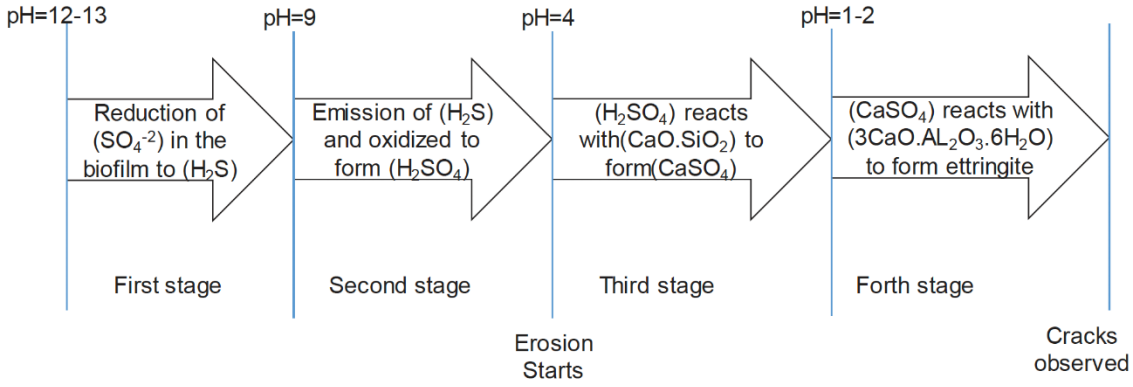

Figure 1. Chemical process of deterioration due to corrosion.

3.2. Multi-Sensor Inspection (MSI) Technology

There are many inspection techniques to inspect a sanitary sewer pipeline such as electro-scan, acoustic emission, CCTV, laser ring, LiDAR, sonar, etc. *(12)*. Typically, municipalities across the world use CCTV for inspection of pipelines. It is the most frequently used, most cost-efficient, and most effective method to inspect the internal condition of a sewer for sewer lines *(13)*. However, CCTV feeds are not able to quantify the defects such as deformation, infiltration, and surface damage, as well as not able to evaluate sulfide-induced corrosion. So new technologies are developed. Other techniques such as pipe penetrating radar (PPR) *(14)* which mainly used for calculating the thickness of pipes and evaluating the bedding condition of pipes *(15)*. Acoustic technologies *(16)* is used to find blockage and/or identifying the presents of lateral pipes. Laser profiling technology provides higher accuracy to identify the deformation such as ovality, and defects as cracks and deposits above the flow line *(17)*. Laser profiling often integrate with other

technologies such as sonar, to be able to detect defects such as deposits (debris) below the flow line *(18)*. However, laser profiling is errors prone when it is monitoring the partially filled pipes, because the laser emitter could be covered by water droplets and scans inaccurate and noisy profiling of the pipe. The multi-sensor inspection equipment has entered the industry as a non-destructive evaluation (NDE) technique to evaluate the pipe condition. LiDAR technology offers an excellent tool for acquiring such data with a fast turn-around time to obtain a high-resolution, high-accuracy point cloud of data (PCD) from the inner wall of the RCPs. Moreover, usually a CCTV camera, which is attached to the same crawler that collects LiDAR data, stores CCTV feeds for further analysis *(19)*. Utilizing LiDAR would clearly present the actual condition of the pipeline such as how much it is corroded or whether there is any deposit. It effectively detects corrosion, debris and ovality *(20)*.

3.3. Probabilistic Deterioration Modeling

Since sanitary sewer mains are buried underground, they could collapse without showing significant warning. Performing proper deterioration models with advanced inspection methods can drastically limit collapses from happening in the future. To provide an accurate residual service life, it is imperative to find a PDF for wall thickness loss (or erosion rate) that best fits the corresponding histograms. One of the most common distributions used in reliability theory is the Weibull distribution *(9)*. This distribution has the capability of estimating the failure of a structure using a small size sample. Weibull distribution can have one, two and three parameters. Equation 7 describes the probability density function for 2- parameters Weibull distribution *(21)*:

$$f(x;\lambda,k) = \begin{cases} \frac{k}{\lambda} * \left(\frac{x}{\lambda}\right)^{k-1} * e^{-\left(\frac{x}{\lambda}\right)^{k}} & x \geq 0 \\ 0 & X < 0 \end{cases} \quad [7]$$

where:

k = the shape parameter;

λ = the scalar parameter ($\lambda > 0$);

Figure 2 shows shape of PDFs for 2-parameter Weibull distribution with different shape and scale parameters.

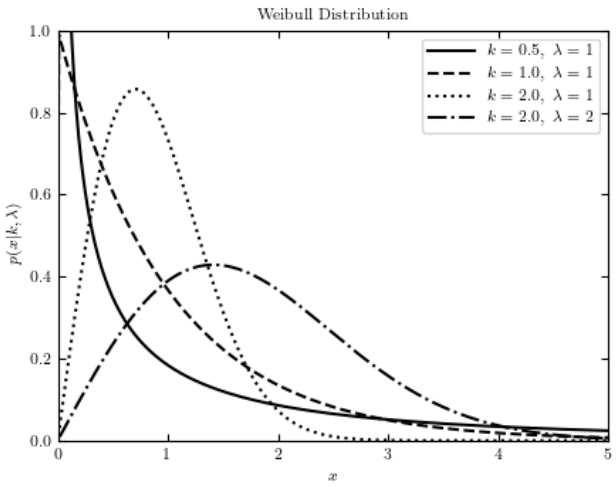

Figure 2. Probability density function of Weibull distribution with different shape *(k)* parameters *(21)*.

In this project a simpler distribution is used. Half Normal distribution will be used to fit the inner wall loss data for each section. Half Normal is a special case of Normal distribution (with the mean of zero). The Half Normal distribution is used for dealing with relationships between measurement errors, introduced by Altman *(22)*. The PDF for the Normal and Half-Normal distributions are shown in Figure 3. The PDF of Half-Normal distribution is shown in Equation 2.

$$f(x,\sigma) = \begin{cases} \frac{2}{\sqrt{2\pi}\,\sigma} * e^{-\left(\frac{x^2}{2\sigma^2}\right)} & x \geq 0 \\ 0 & x < 0 \end{cases} \qquad [8]$$

where:

σ = Standard deviation;

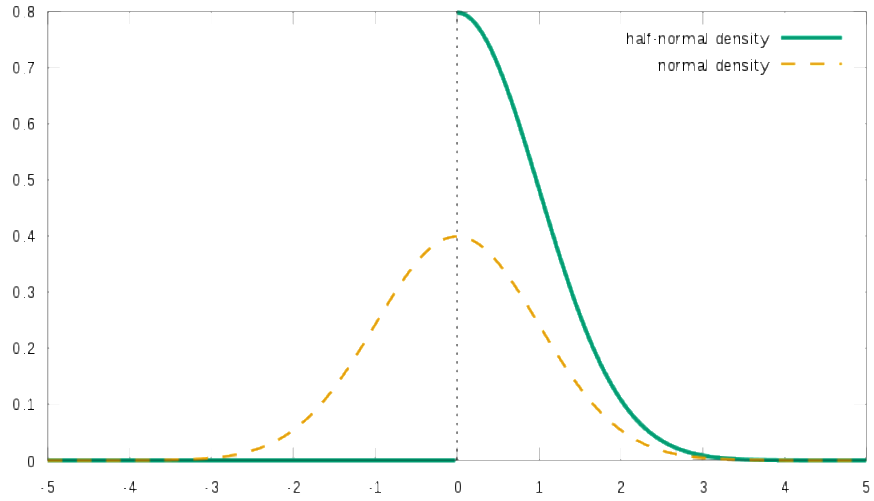

Figure 3. PDFs for Normal Distribution (with zero mean and std of 1) and Half-Normal Distribution (std. of 1) *(22)*.

4. METHODOLOGY

4.1. Pipeline specification, Inspection Device, and Software Program Used

Ten different RC sanitary sewer pipelines are selected for the purpose of current study, resulting in a total of 2,901 linear foot of pipelines inspection data using LiDAR measurements and CCTV feeds. Figure 4 shows screenshots of the 10 selected RCPs. The labels below each figure will be used for identification and properties of the inspected pipes.

BW230002-BW230001

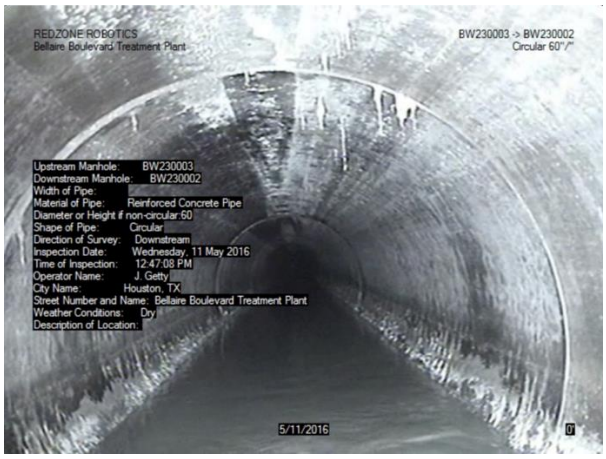

BW230003-BW230002

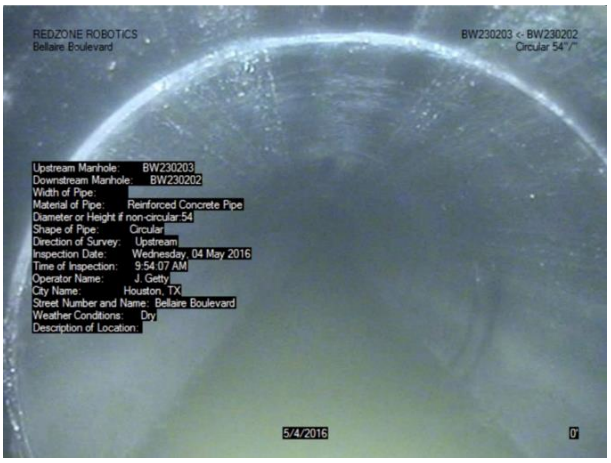

BW230203-BW230202

BW230004-BW230003

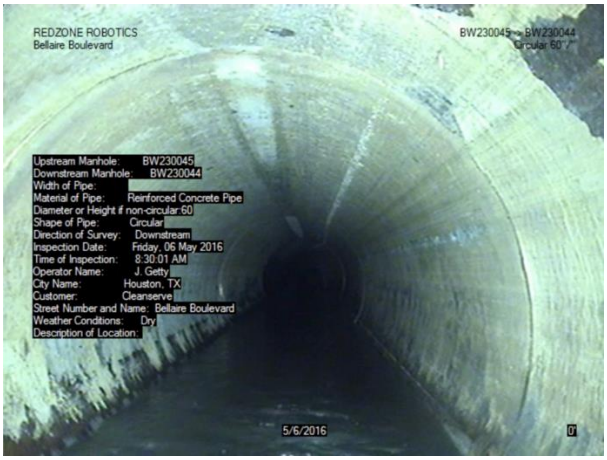

BW230045-BW2300044 ***BW230046-BW230045***

BW230066-BW2300065 ***BW230011-BW230010***

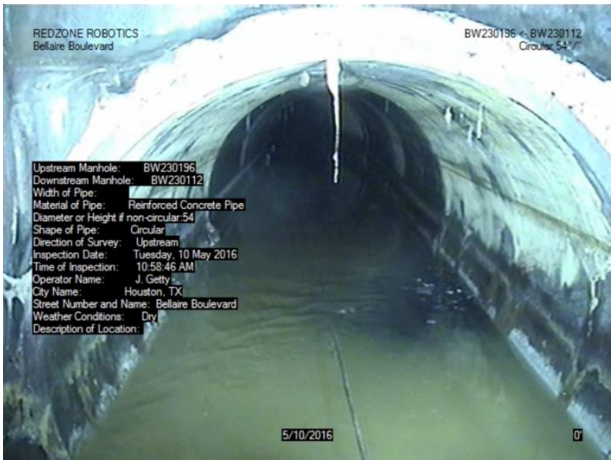

BW230196-BW2300112 ***BW230199-BW230198***

Figure 4. Screenshots of CCTVs from the 10 different RC sanitary pipelines.

The LiDAR measurements in this study were obtained from a field inspection using the MSI equipment from RedZone Robotics *(20)* with the collaboration of CSER/SPI at UTA. The robot typically crawls into a partially filled pipelines and record videos from the inside of the pipeline as it moves from one manhole to the other. Figure 5 shows the MSI robot used in this research. At each 5-ft section, the robot scans the inside wall of RC pipeline using the LiDAR measurements. The collected point cloud of data (raw data) is in spherical coordinate (r, θ, φ). All the procedures for processing LIDAR information, obtaining current corrosion levels and performing the probabilistic service life prediction is performed using a code written in MATLAB. The algorithms is explained thoroughly in the following sections.

Figure 5. MSI RedZone robot *(20)*.

For the sake of brevity, for the rest of the report line numbers will be used instead of their code names shown in Figure 4. Table 1 shows the selected pipelines and their properties including age, diameter, slope and inspected length.

Table 1.The properties of selected RC Pipeline.

Line number	Name of the line	Age (month)	Diameter(in)	Slope(%)	Length(Ft)
1	'BW230002-BW230001'	338	60	5	345
2	'BW230003-BW230002-down'	338	60	5	190
3	'BW230203-BW230202-up'	338	60	5	30
4	'BW230004-BW230003-down'	339	60	5	260
5	'BW230045-BW230044-down'	339	54	5	220
6	'BW230046-BW230045-down'	339	54	6	480
7	'BW230066-BW230065-down'	339	54	6	437
8	'BW230111-BW230110-up'	339	54	6	317
9	'BW230196-BW230112-up'	339	54	6	205
10	'BW230199-BW230198-up'	339	54	6	417

4.2. The Data Collection properties

The LiDAR scans in the form of point clouds (raw data), are available for each 5-ft section of the pipeline. The LiDAR scans beyond the 5-ft show significant scattering and are therefore omitted. For instance, the line number 2 has a length of 250 ft. As a result, there are 250/5=50 different scans available. In this study, the proposed methodology is applied for each individual scans of 5-ft section.

The output data of the MSI robot (i.e., the raw data) are in spherical coordinates. Therefore, each point of data has radial distance r (in mm), inclination angle (in degree, $0< \boldsymbol{\varphi} <180$), azimuth angle (in degree, $0<\theta<360$).

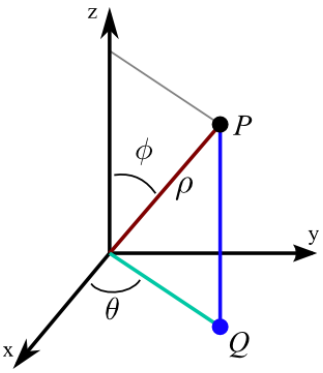

Figure 6. Spherical coordinate space vs. Cartesian coordinate system.

4.3. Modeling Assumptions

- Inner wall concrete cover is assumed to be uniform for all sewer lines. It is expressed as a single value of 1 inch according to ASTM C76 *(23)*.
- The corrosion rate is assumed to be constant throughout the life span of pipelines.

4.4. Proposed Algorithm

In this section the automated algorithm is thoroughly explained. To illustrate the process, line 1, first 5-ft section is selected.

4.4.1. Filtering

First, the spherical coordinate $(\boldsymbol{r}, \boldsymbol{\theta}, \boldsymbol{\varphi})$ is converted to Cartesian coordinate (x,y,z) using Equation 9.

$$x = r\cos(\theta)\sin(\boldsymbol{\varphi})$$
$$y = r\sin(\theta)\,sin(\boldsymbol{\varphi})$$
$$z = r\,cos(\boldsymbol{\varphi}) \qquad [9]$$

where:

r = the radial distance (mm);

θ = the azimuth angle (Degree);

$\boldsymbol{\varphi}$= the inclination angle (Degree);

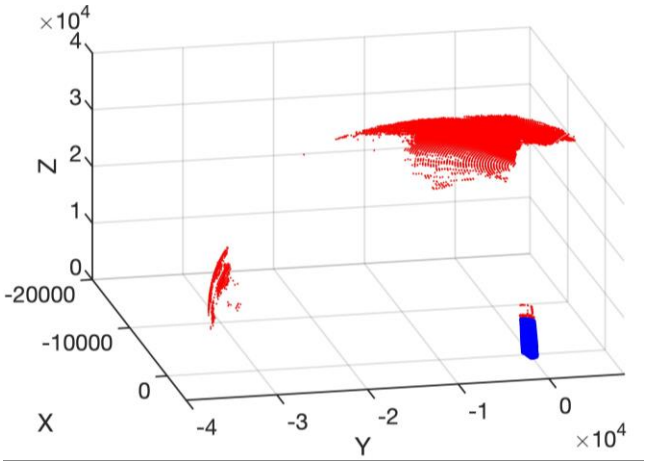

Figure 7. Unfiltered data in Cartesian space.

Figure 7 shows the unfiltered data in Cartesian space. The blue object at the center of the sphere is the pipeline, while the remaining blue data points are noises. The filtering is applied in two steps as follows:

4.4.1.1. Global filtering

The robot is located at the start of the pipeline (at center of the sphere). Since the diameter and length of the pipe are 60 in. (1524 mm), and 5 ft (1524 mm), respectively, points with a radial distance 500 < r < 2000 mm are included in the transformation using Eq.3. The results are shown in Figure 8.

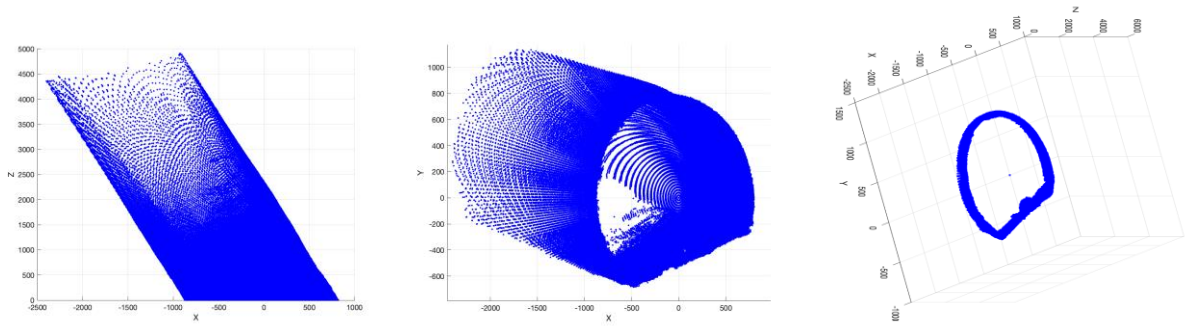

(a) **(b)** **(c)**

Figure 8. Cloud of points after global filtering: (a) Z-X view, (b) X-Y view, and (c) 3-D view.

4.4.1.2. Water Level Filtering:

Water level data is removed by finding the range of azimuth angle θ that contains the bottom circle of the pipe. The range of azimuth angle is shown in Equation 10.

$$\begin{cases} \theta_{min} < \theta < \theta_{Max} & if\ \boldsymbol{\varphi} \leq 0 \\ \theta_{min} + 180 < \theta < \theta_{Max} + 180 & if\ \boldsymbol{\varphi} > 0 \end{cases} \quad [10]$$

By trial and error, the lower and upper bounds for azimuth angle are found to be θ_{min} = [0,15] and θ_{Max} = [155,170], respectively. Once these two angles are found for the first section, the same constraint are applied to all the other 5-ft sections within a line. Similarly, the points for which the azimuth angle are in the correct range of Equation 10 are included for transformation using Equation 9. Figure 9 shows the final shape of data after the two phases of filtering is applied.

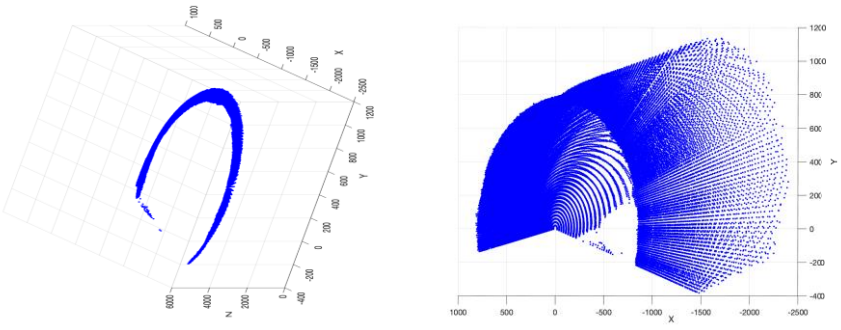

(a) **(b)**

Figure 9. Data after filtering of water level soise: (a) 3-D view and (b) Y-X view.

It is worth mentioning that in each scan of the so-called 5-ft section, more than 5-ft length of the pipe is scanned (it is about 15-ft). So, after aligning the pipe, the extra data beyond 5 ft. is trimmed.

4.4.2. Alignment

One of the challenges in using the LiDAR measurements is that the orientation of the data is unknown. To evaluate the corrosion rate consistently, it is necessary that all the point cloud of data for the 5-ft sections are rotated consistently to be oriented in the same direction. Alignment is done in two steps:

1. For each section, reference line is found by selecting the points along the length of the pipe. This reference line was found by trial and error and as a result the following constraints are applied to the raw data conversion when using Eq.3:

$$340 < \theta < 341 \quad \& \quad \boldsymbol{\varphi} \leq -30$$

This angle is found to be the same for all sections of the 10 sewer lines. Figure 10 shows the reference line for line 1, section 1.

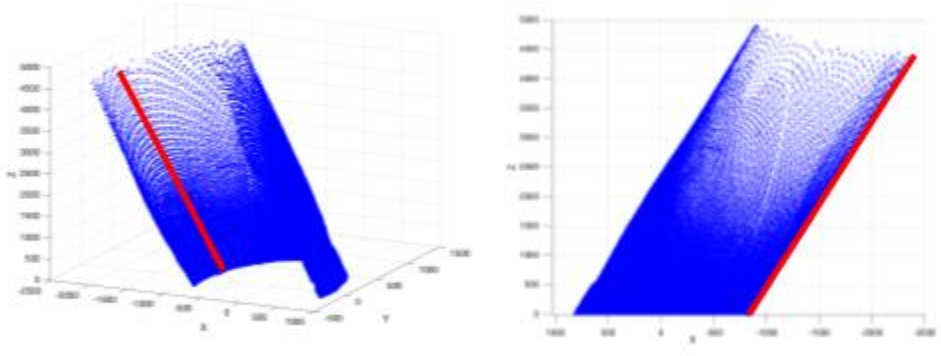

(a) **(b)**

Figure 10. Reference points for line 1, section 1: (a) 3-D view and (b) Z-X view.

2. Finding the eigenvector for the reference line: eigenvalue decomposition is the best tool for calculating the direction of an arbitrary line in 3-D space. To apply this method, variance/covariance matrix of the selected reference points is calculated as follows:

a) Assume matrix of our reference points is:

$$\begin{bmatrix} x_1\ y_1\ z_1 \\ x_2\ y_2\ z_2 \\ x_3\ y_3\ z_3 \\ \vdots \\ x_N\ y_N\ z_N \end{bmatrix}$$

b) Calculate the mean of dimensions (each column): $[\bar{X}\ \bar{Y}\ \bar{Z}]$

c) Subtract each dimension (columns) from its means to create centered data:

$$\begin{bmatrix} (x_1-\bar{X})(y_1-\bar{Y})\ (z_1-\bar{Z}) \\ (x_2-\bar{X})(y_2-\bar{Y})\ (z_2-\bar{Z}) \\ (x_3-\bar{X})(y_3-\bar{Y})\ (z_3-\bar{Z}) \\ \vdots \\ (x_N-\bar{X})(y_N-\bar{Y})\ (z_N-\bar{Z}) \end{bmatrix}$$

d) Create variance covariance matrix of centered data:

$$A = \begin{bmatrix} \sum_{i=1}^{N}(x_i-\overline{X})^2 & \sum_{i=1}^{N}(x_i-\overline{X})(y_i-\overline{Y}) & \sum_{i=1}^{N}(x_i-\overline{X})(z_i-\overline{Z}) \\ \sum_{i=1}^{N}(y_i-\overline{Y})(x_i-\overline{X}) & \sum_{i=1}^{N}(y_i-\overline{Y})^2 & \sum_{i=1}^{N}(y_i-\overline{Y})(z_i-\overline{Z}) \\ \sum_{i=1}^{N}(z_i-\overline{Z})(x_i-\overline{X}) & \sum_{i=1}^{N}(z_i-\overline{Z})(y_i-\overline{Y}) & \sum_{i=1}^{N}(z_i-\overline{Z})^2 \end{bmatrix}$$

e) Eigenvalue decomposition is done using built-in function in MATLAB (*eig).*

[V,D] = eig(A) produces a diagonal matrix *D* of eigenvalues and a full matrix V whose columns are the corresponding eigenvectors so that *A*V = V*D.* The column corresponding to the larger eigenvector (*D*) is the direction of the pipe in 3-D space.

$$v = \begin{bmatrix} \mathrm{v}_{3,1} \\ \mathrm{v}_{3,2} \\ \mathrm{v}_{3,3} \end{bmatrix}_{3\mathrm{x}1}$$

The rotation of the cloud of points is done using the MATLAB code provided by [24]. It creates a roto-translation matrix that rotates vector *v* to the constant direction which is *i=[0,0,1]'* (i.e., the unit vector of Z-direction). From Figure 11, the red points are the original data, and the blue points are the aligned data.

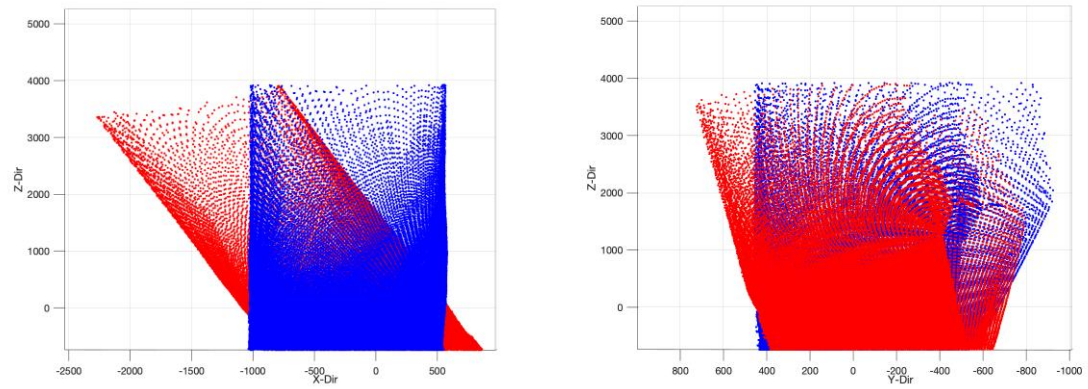

(a) **(b)**

Figure 11. Rotating the cloud of point data in a constant direction: (a) Z-X view and (b) Z-Y view.

The final shape after trimming the 5-ft section is shown Figure 12.

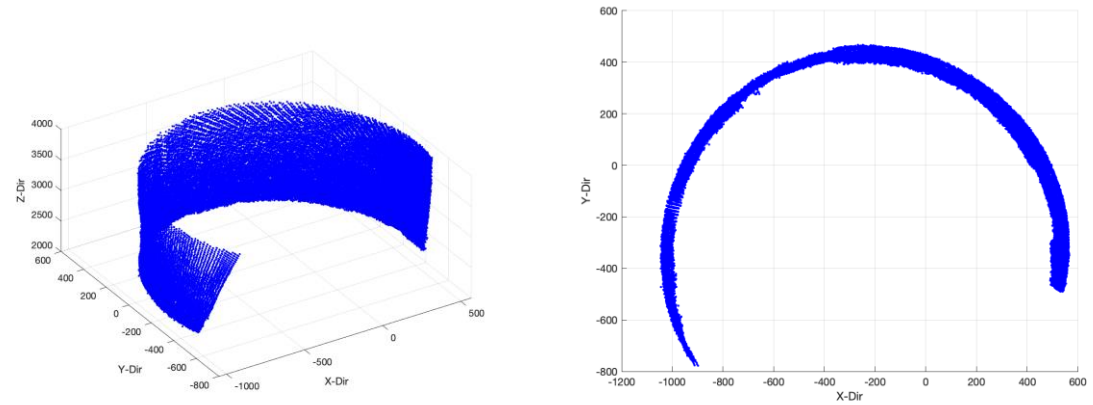

(a) **(b)**

Figure 12. Filtered, aligned, and trimmed point cloud of data: (a) 3-D view and (b) Y-X view (cross section).

4.4.3. Evaluate Corrosion Rate

The points presented in Figure 12 are used for calculating the inner wall thickness loss of each section. As mentioned earlier, each 5-ft length of the cylinder is divided into 60 rings with a thickness of 1-in (25.4 mm). One inch thickness (Z direction) is negligible compared to the diameter of the pipe (54”-60”); therefore, instead of working in 3-D space (X-Y-Z), each ring can be analyzed in 2-D space (X-Y) (Figure 12). So, instead of using a time-consuming cylinder-fitting method in 3-D space that is subject to user error, a circle fitting method in 2-D space can be used instead. The corrosion rate is calculated for each 1-in ring as follows:

a) To ensure that the data is centered at (x=0, y=0) and completely aligned, the procedure explained in section 4.4.2 part 2, is performed for each ring; the direction of a ring is used instead of the reference points of line. Figure 13 shows the points cloud of data for the first 1-in ring of the line 1, section 1; it is shown in cylindrical coordinate for better representation.

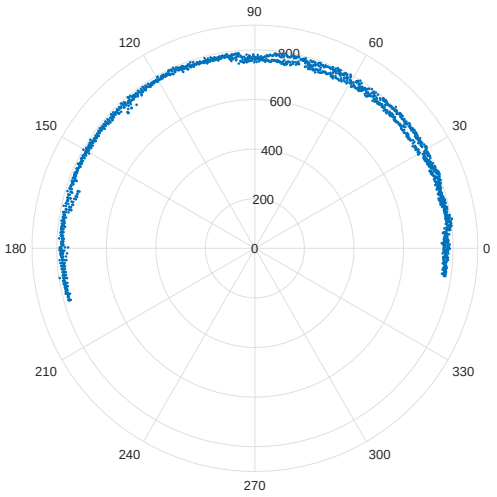

Figure 13. 1-in ring of point cloud of data (mm, degree).

b) A circle is then fitted to the ring using Landau method provided by Sumith *(25)*. Figure 14 shows the fitted circle along with the filtered data.

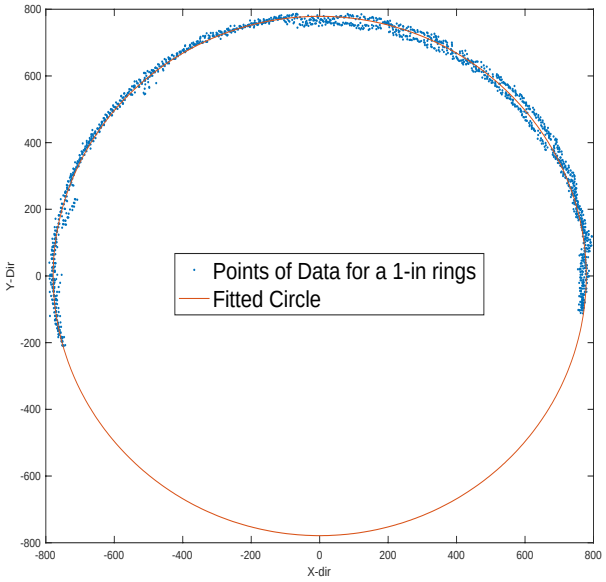

Figure 14. Fitted circle for a ring of points.

c) For each point of the 1-in rings (i.e., the blue points in Figure 14), the loss is calculated by how much a point is located away from the fitted circle in positive direction (+). The deposit is calculated by the same method but having the opposite direction (-) (Figure 15)

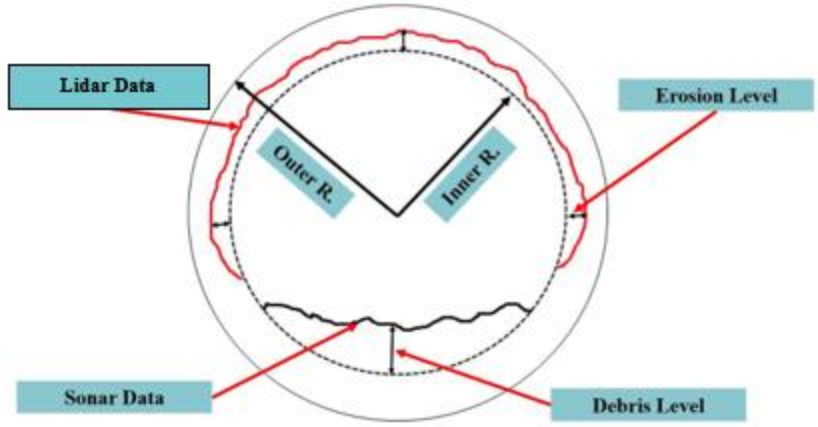

Figure 15. Definition of loss and deposit.

4.4.4. Fitting the best distribution

After calculating the wall-thickness losses, the best probability density function is selected among 11 different distributions. These selected PDFS are:

1. Normal distribution;

2. Rayleigh distribution;

3. Rician distribution;

4. Stable distribution:

5. Half Normal distribution;

6. Nakagami distribution;

7. Exponential distribution;

8. Gamma distribution;

9. Birnbaum-Saunders distribution;

10. Weibull distribution;

11. Inverse Gaussian distribution.

These distributions are among the most famous distributions used for characterizing deterioration of structures. Goodness of fit is measured by comparing R^2 values for fitted line to QQ-plots of each 1″ rings. Figure 16 shows the results for the distribution fitting algorithm.

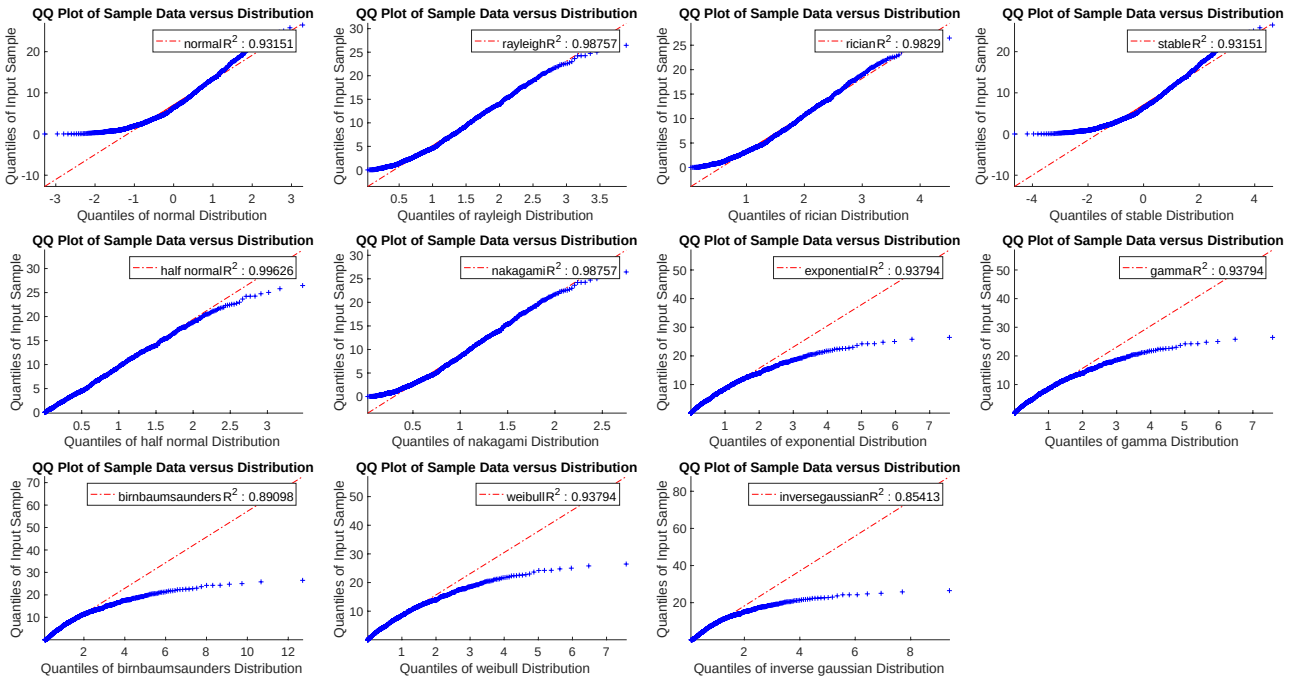

Figure 16. Results for fitting different distribution to the losses of line 1.

For the sake of brevity, results for the remaining lines are show in Appendix B. Figure 16 shows that it is reasonable to use Half Normal distribution (with mean of zero) for the losses. The results shows that the data could be following Exponential distribution or Weibull distribution as well; however, it is easier to use Half Normal distribution because it is dependent on only one parameter (i.e., standard deviation and the mean of zero). Figures 17-18 shows the top 3 distributions that their R^2 values are closest to 1. It can also be verified visually that Half Normal distribution is the best fit.

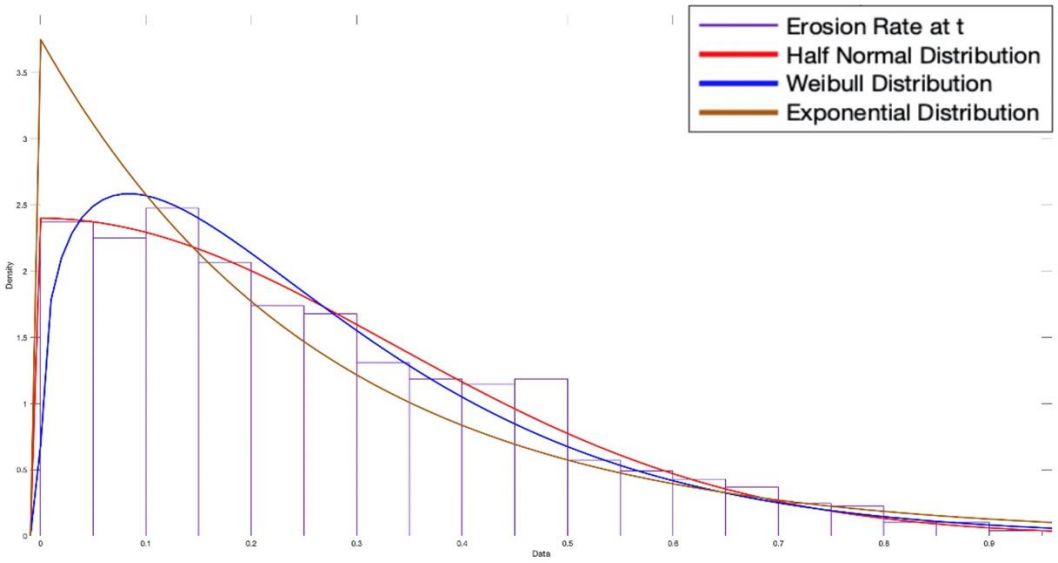

Figure 17. Fitting three different probability density function on erosion data.

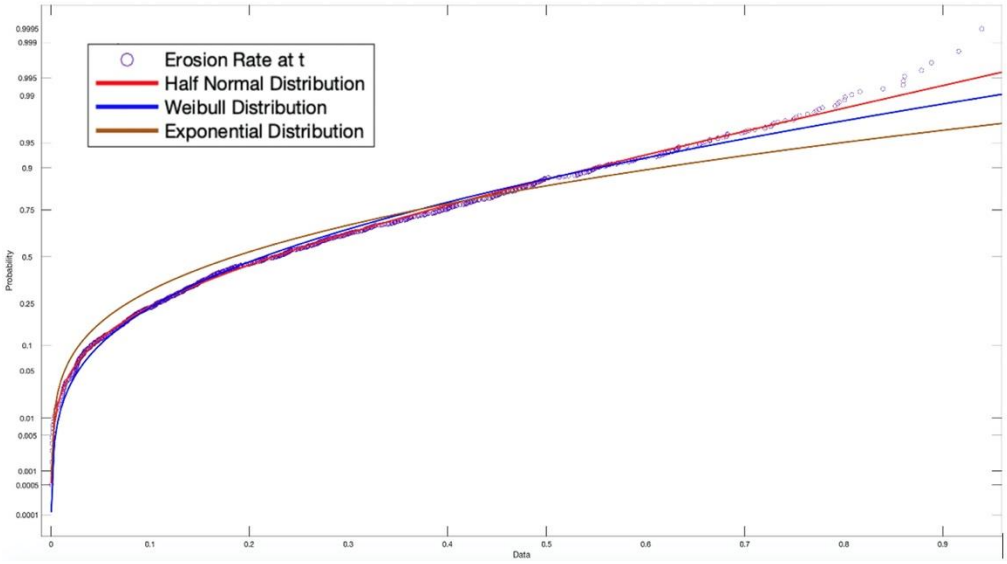

Figure 18. Probability plots of 3 different fit on erosion data.

These results are used for the probabilistic residual service life estimation of pipelines as elaborated in section 5. Also, the difference between different distributions in terms of life expectancy is shown.

It should be noted that to the best of the knowledge of the research team, the above procedure has been done manually up to now, which makes the procedure less consistent and dependent on the skills of the user. Therefore, the proposed framework shall result in a more consistent and uniform condition assessment of the RCP sewer lines.

4.4.5. Calculating Life Expectancy of Pipeline

After finding the loss values, the erosion rate is calculated according to Equation 11.

$$\text{Er}\left(\frac{\text{mm}}{\text{year}}\right) = \frac{\text{Erosion at the time of inspection}}{\text{Age of the section at the time of inspection}} \quad [11]$$

It should be noted that erosion rate is calculated for each point not the average loss of rings. Since erosion is a deterioration phenomenon, it is assumed that it increases at a constant rate as the time elapses.

Life expectancy of each ring is calculated using the two methods:

4.4.5.1. Probability of Exceedance

This concept is integrated by the concept of limit state (G), described in Equation 12.

$$G(t) = R(t)\text{-}E(t) \quad [12]$$

where R is resistance defined as concrete cover of *1* inch; the cover protects the reinforcement from corrosion by isolating it from the surrounding environment. E is action considered as corrosion rate; t is the age of the pipeline at the time of inspection. By this definition failure occurs when the action E overcomes the resistance R. In addition, E at each point of the ring is different,

so the erosion at *t* is presented as a random variable that follows the best fit distribution function (e.g., Half Normal).

The probability of failure of each ring at *t* is the area bounded by the probability density function (action) and the concrete cover in which the action is greater than the resistance. According to the basic definition of probability, probability of failure is the area under the probability density function. From Eq. 6, probability of failure is the area under the curve beyond 1 toward infinity as shown in Equation 13.

$$P_f = \int_1^{\infty} f(x)dx \qquad [13]$$

Finally, the service life is estimated as described hereafter. The service life is defined as the time at which the structure requires rehabilitation and maintenance; however, this does not necessarily reflect collapse of that structure. In this study the erosion rate (Equation 12) is used along with probability of failure concept (Equation 13) to estimate the service life of pipes. Using the age of the pipe at the time of inspection, the residual service life of the pipe is calculated according to Equation 14.

$$P_f\,(E(t)>1) \qquad [14]$$

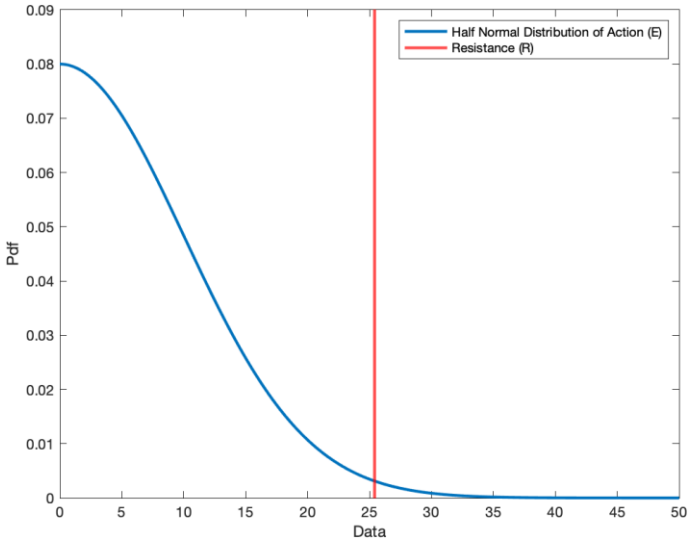

Figure 19. Probability of exceedance for erosion (half normal distribution) at *t*.

This process is repeated for 300 consecutive number of years; the service life is defined as a year in which the value of Equation 11 is more than 0.10. In other word, this is the remaining life (year of maintenance) of ring with 90 percent confidence interval.

4.4.5.2. X-Intercept Method

This method uses the average of concrete wall thickness losses (section 4.4.3, part c) at the time of inspection, assuming that corrosion rate is constant.

The initial cover (C_0) in Figure 20 is assumed to be 1 inch (25.4 mm). In this method the service life (t_{SL}) is calculated by finding the x-intercept and a line which passes through initial cover and mean remaining cover (μ_c) at time of inspection (t_{insp}).

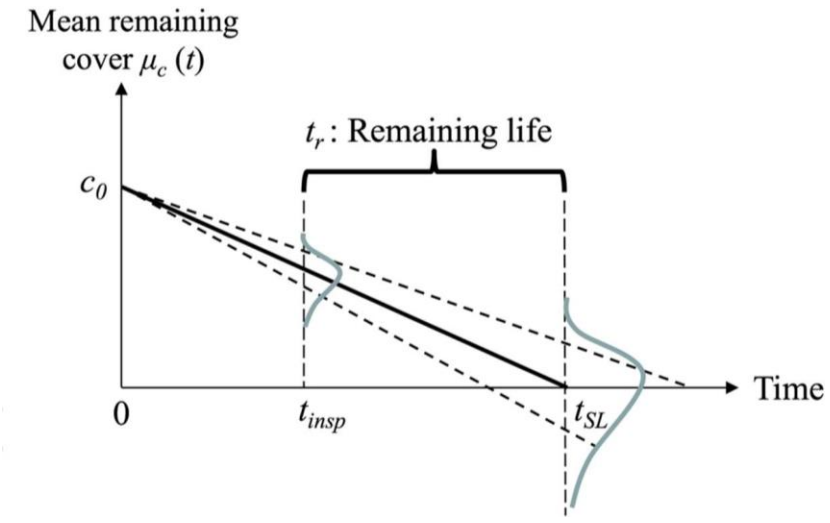

Figure 20. Calculation remaining life using x-intercept method.

In the next section the residual service life of the inspected sewer lines will be shown. Based on the decision makers' resources, the results could be presented at different scales, whether for small 1-inch rings, 5-foot sections, or even for the whole inspected line (M-M).

5. ANALYSIS AND FINDINGS

5.1. Residual Service Life for each 5-ft Section

Using the proposed framework, the residual service life of the pipelines is presented for each 5-ft sections. Figures 21-30 show the results for the 10 selected RC sanitary sewer pipeline using 2 different methods discussed in the previous section 4 (Section 4.4.5). It should be noted that "Method 1" denotes as the method of probability of exceedance (Section 4.4.5.1), and "Method 2" is method of X-intercept (Section 4.4.5.2).

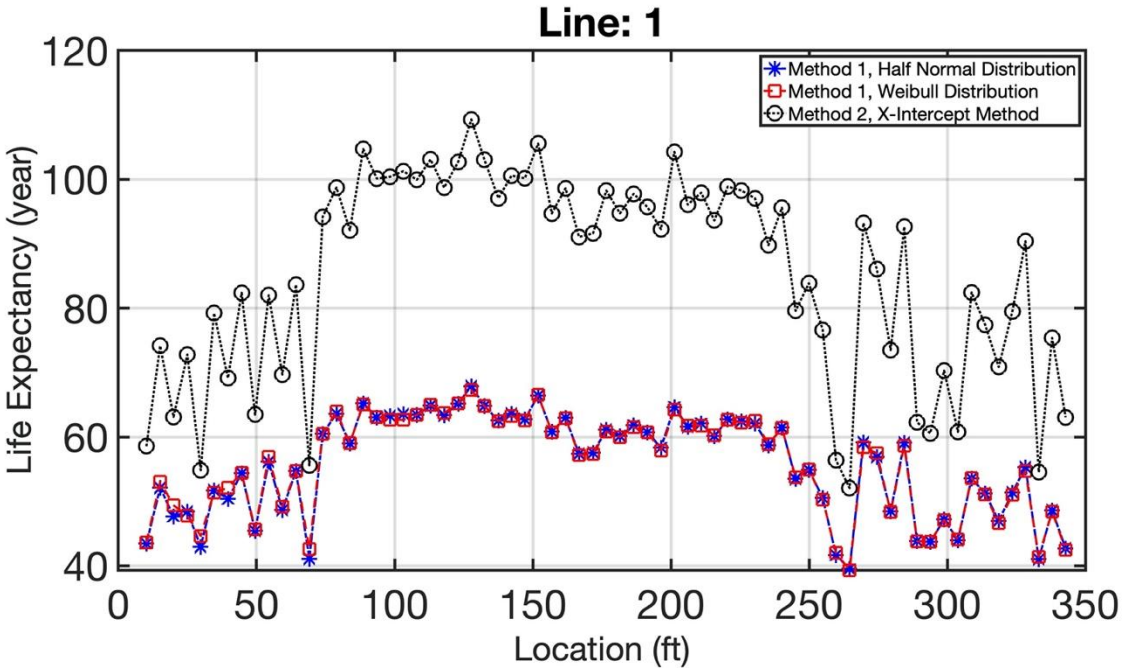

Figure 21. Comparison of life expectancy for line 1.

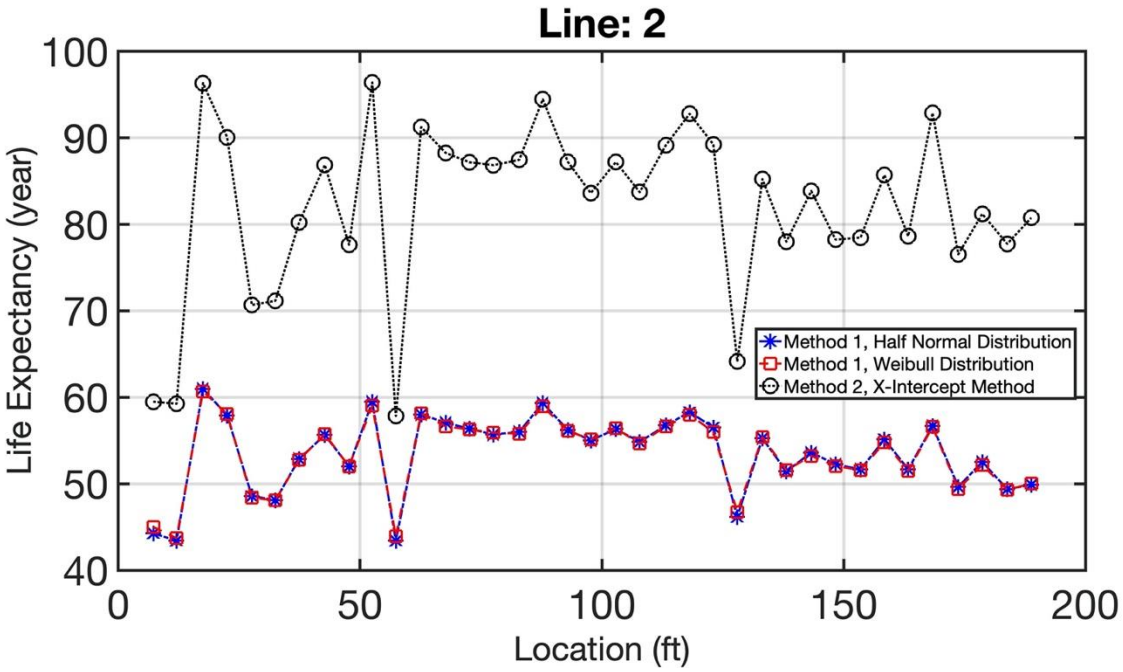

Figure 22. Comparison of life expectancy methods for line 2.

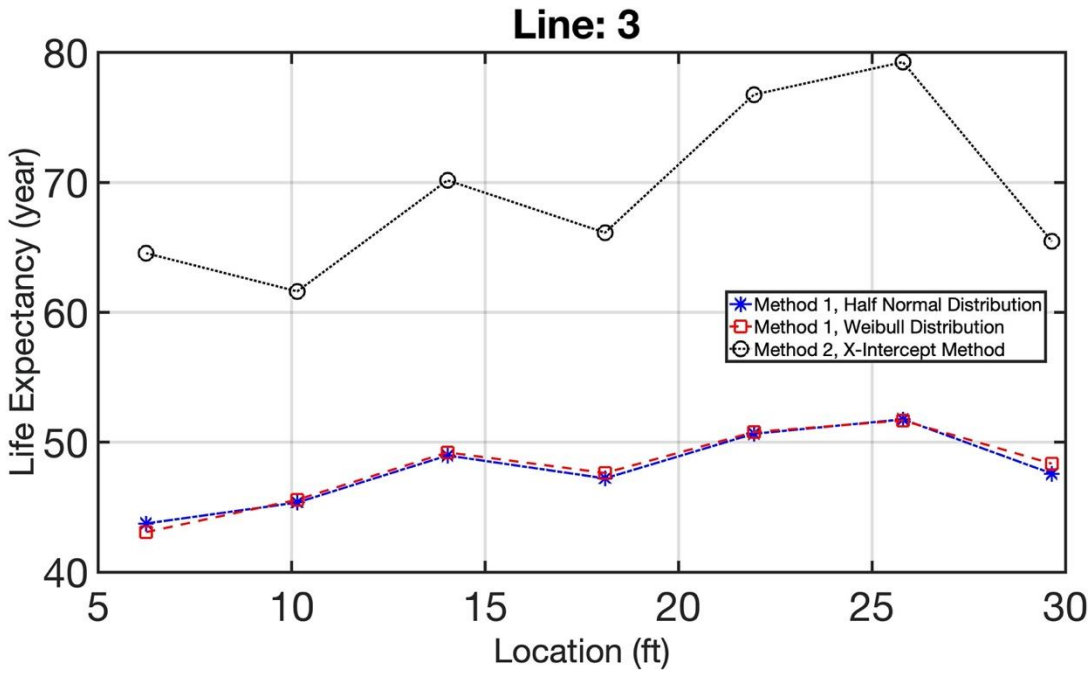

Figure 23. Comparison of life expectancy methods for line 3.

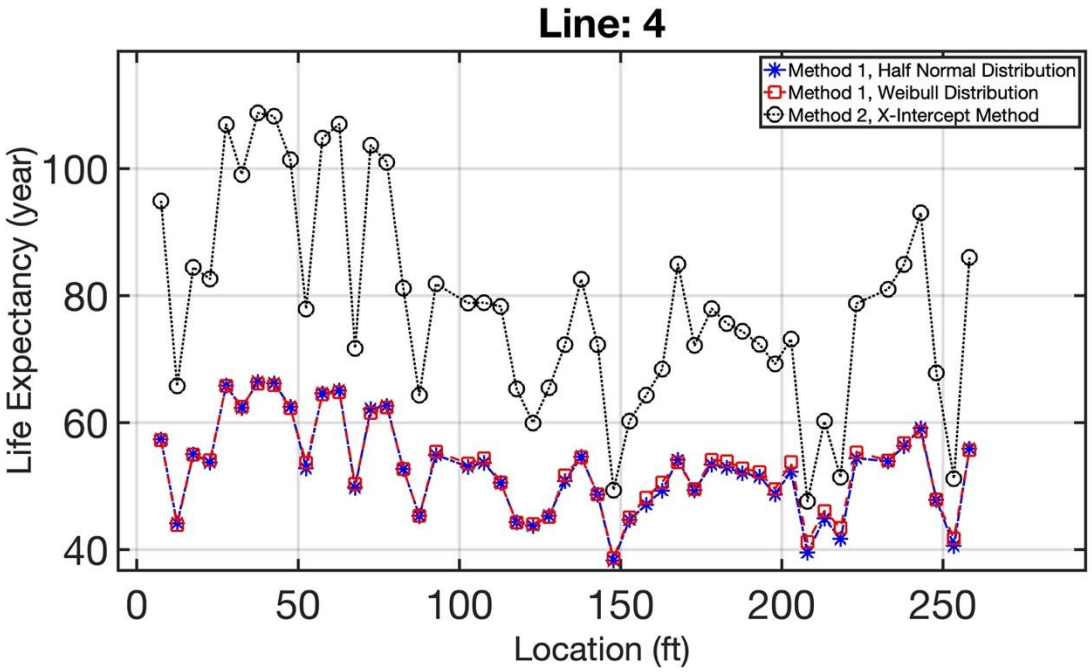

Figure 24. Comparison of life expectancy methods for line 4.

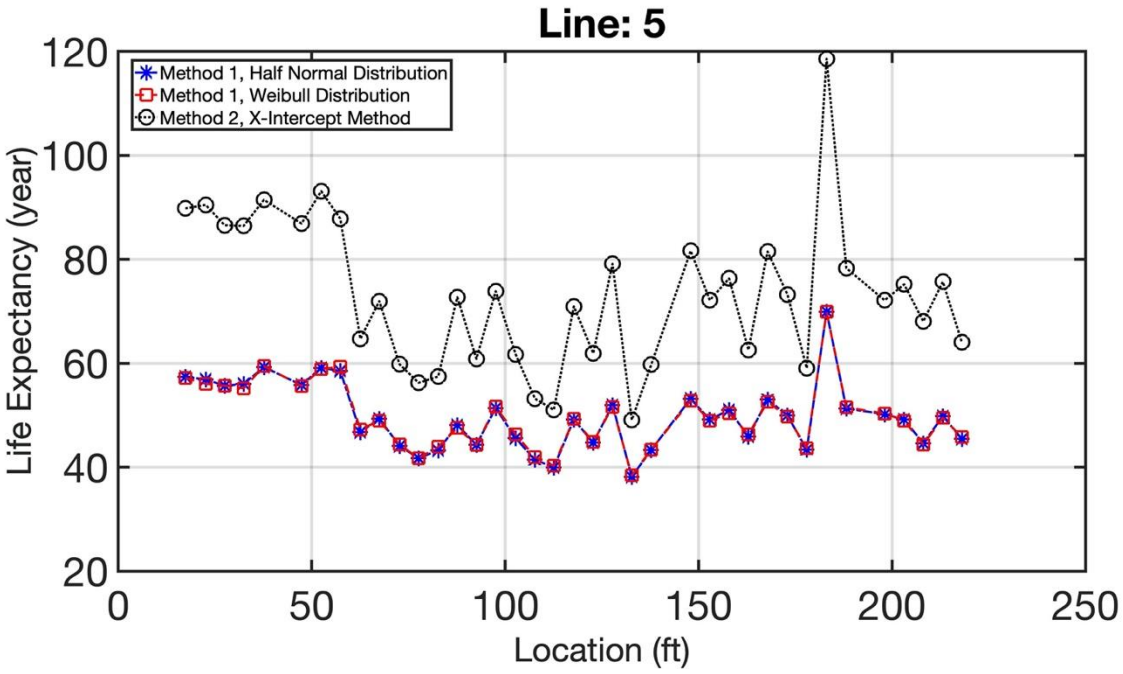

Figure 25. Comparison of life expectancy methods for line 5.

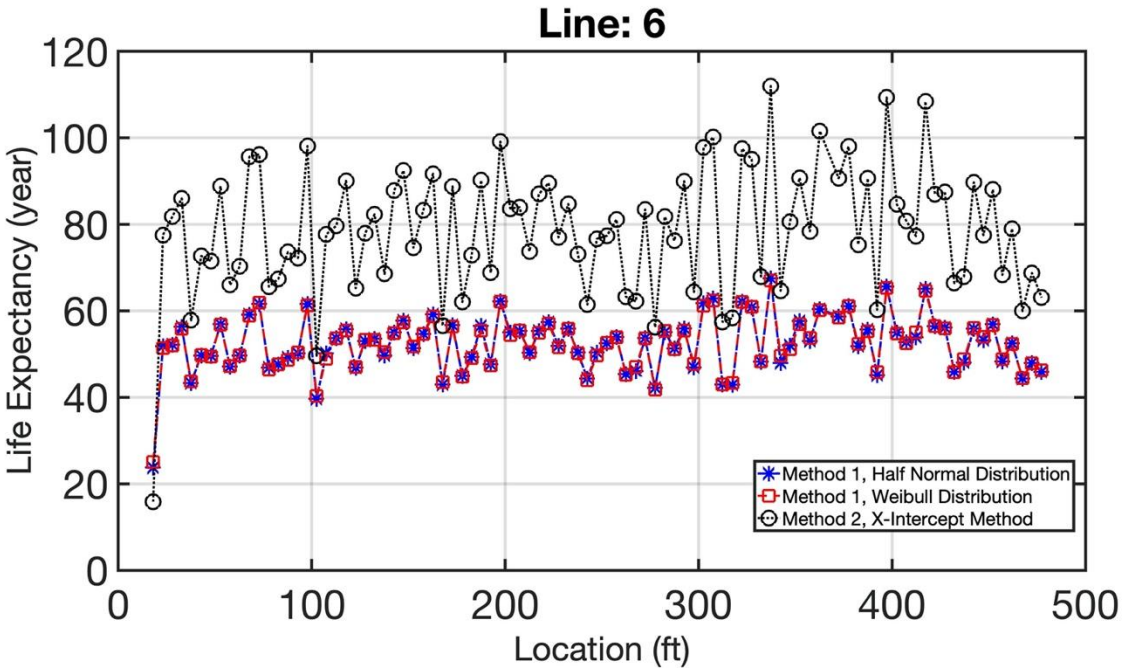

Figure 26. Comparison of life expectancy methods for line 6.

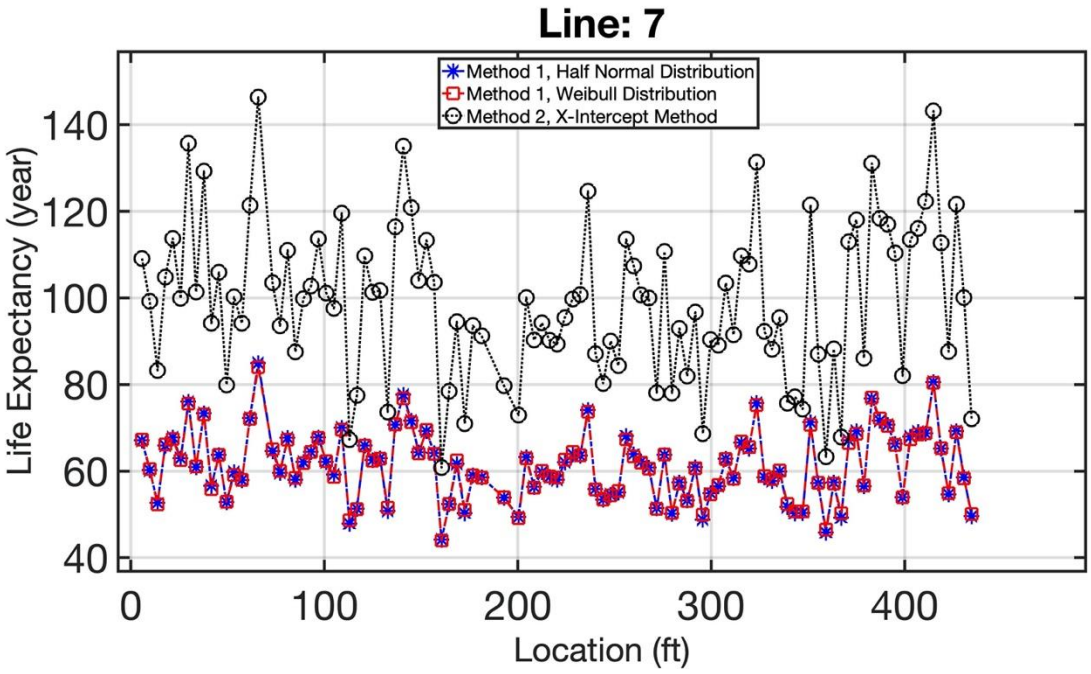

Figure 27. Comparison of life expectancy methods for line 7.

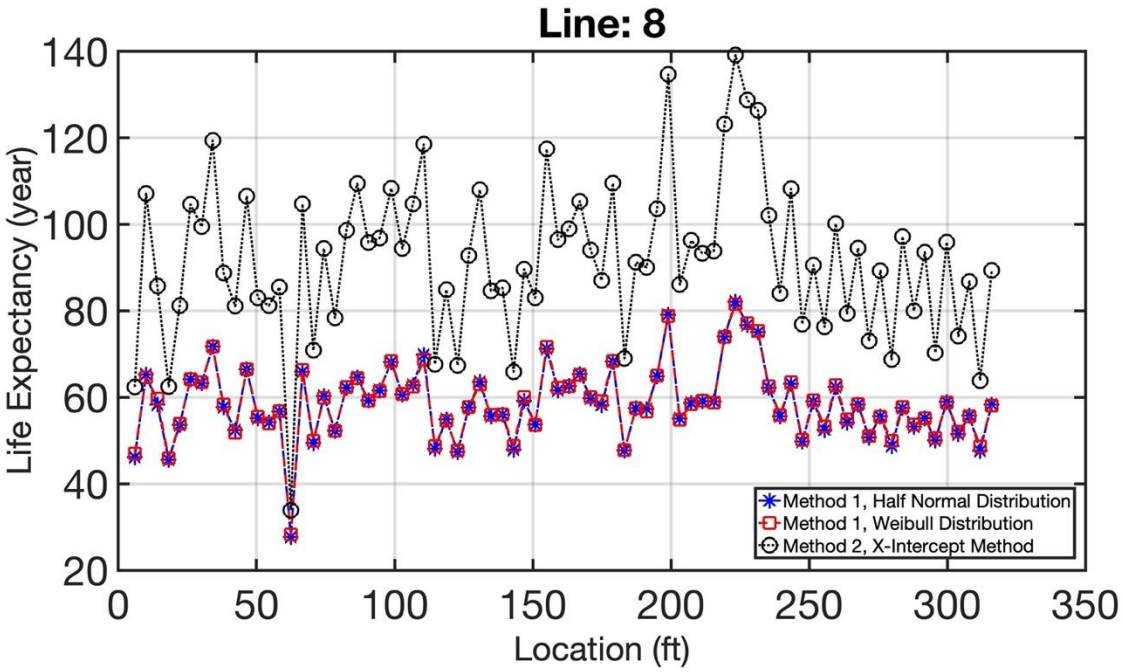

Figure 28. Comparison of life expectancy methods for line 8.

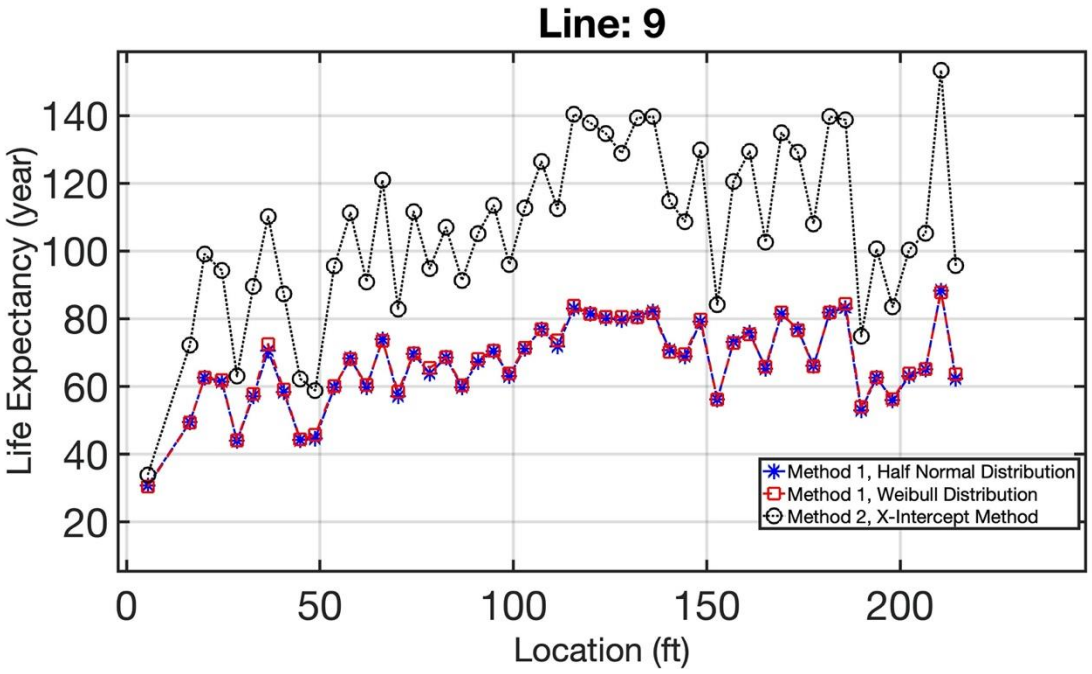

Figure 29. Comparison of life expectancy methods for line 9.

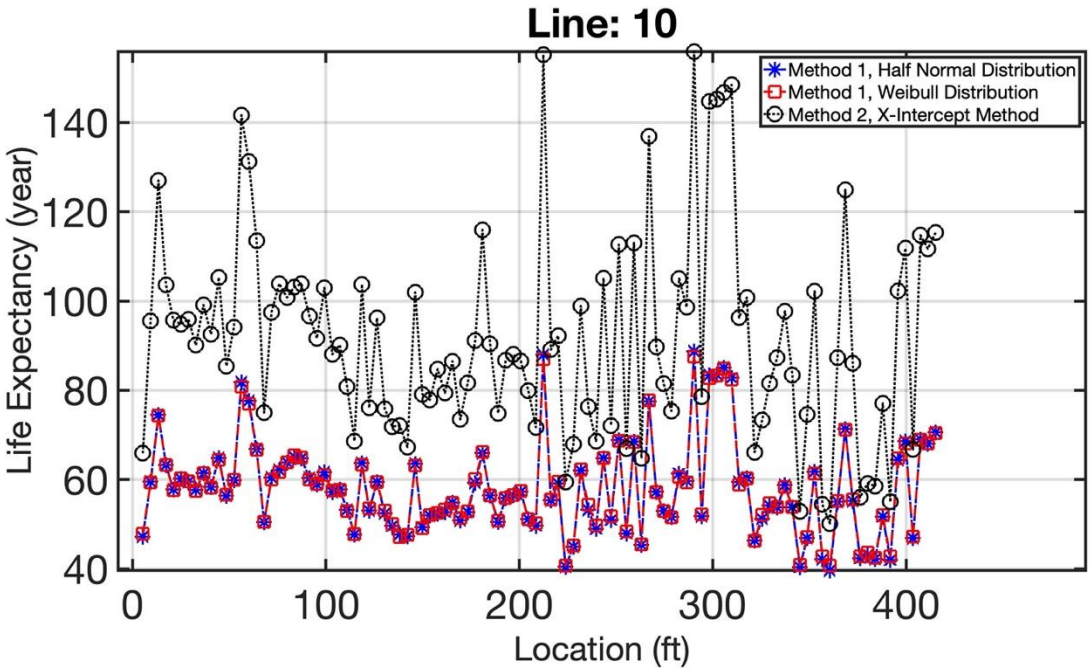

Figure 30. Comparison of life expectancy methods for line 10.

Figures 21-30 show a consistency between the Half-Normal distribution and Weibull distribution and is therefore, the best choice for modeling the erosion rate with uncertainty, since it requires knowing only the standard deviation.

5.2. Simplified approach for Pipeline Assessment

For the matter of simplicity, instead of working with the time consuming and long process of finding the life expectancy, the only parameter of Half Normal distribution (i.e., standard deviation) for the wall losses (not the erosion rate) will be plotted with respect to each location of each 5-ft section. Figure 31-40 shows the results.

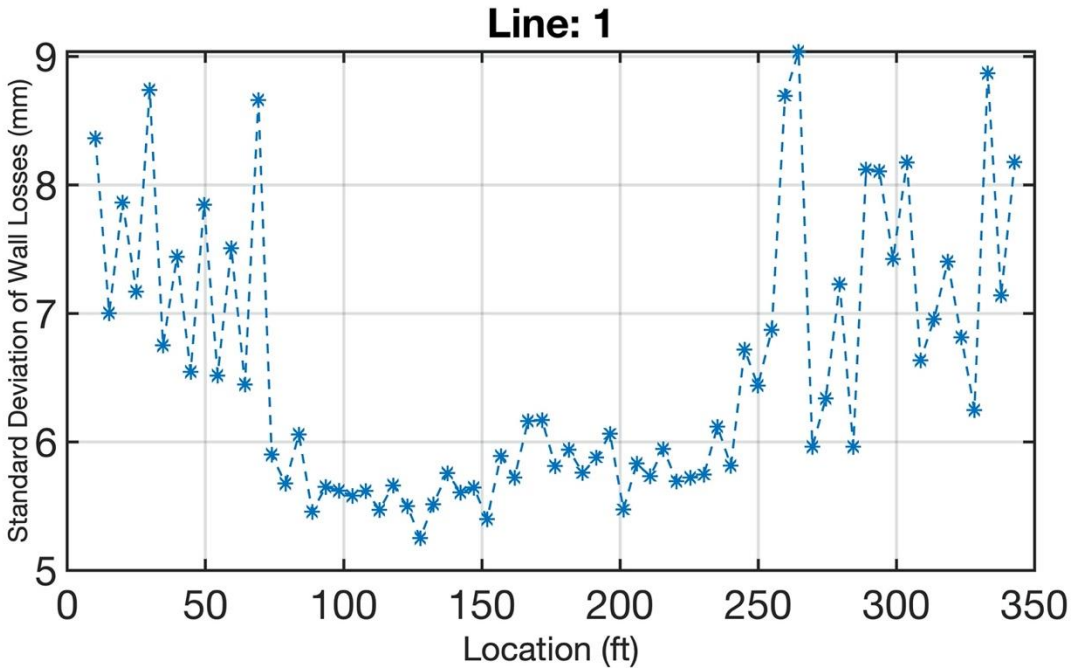

Figure 31. Comparing Half Normal standard deviation of losses for line 1.

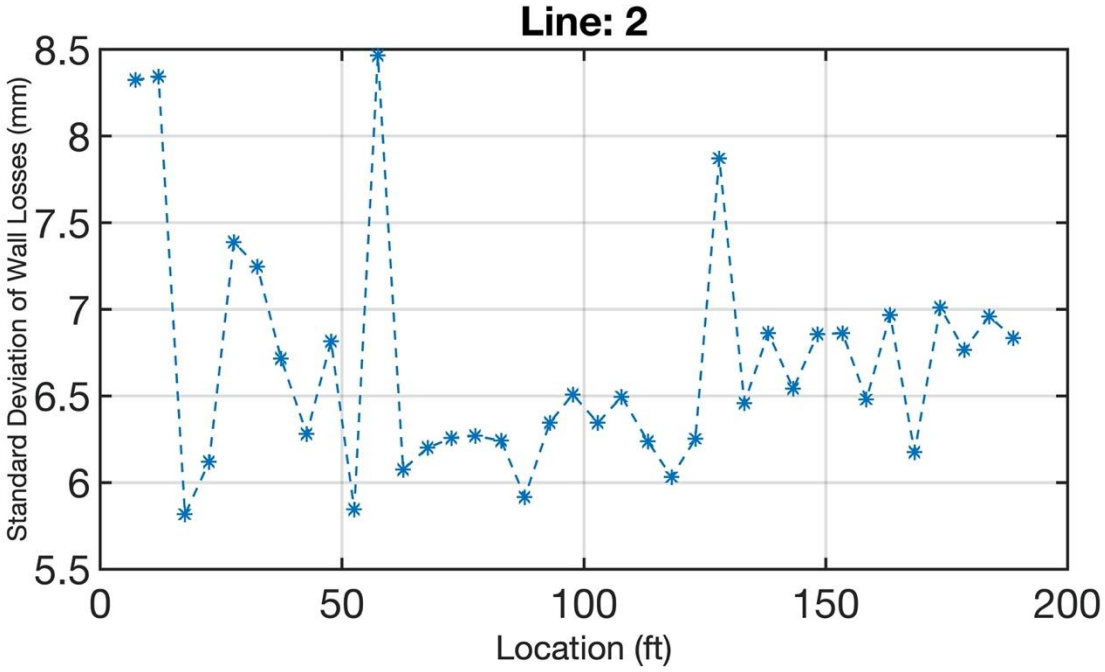

Figure 32. Comparing Half Normal standard deviation of losses for line 2.

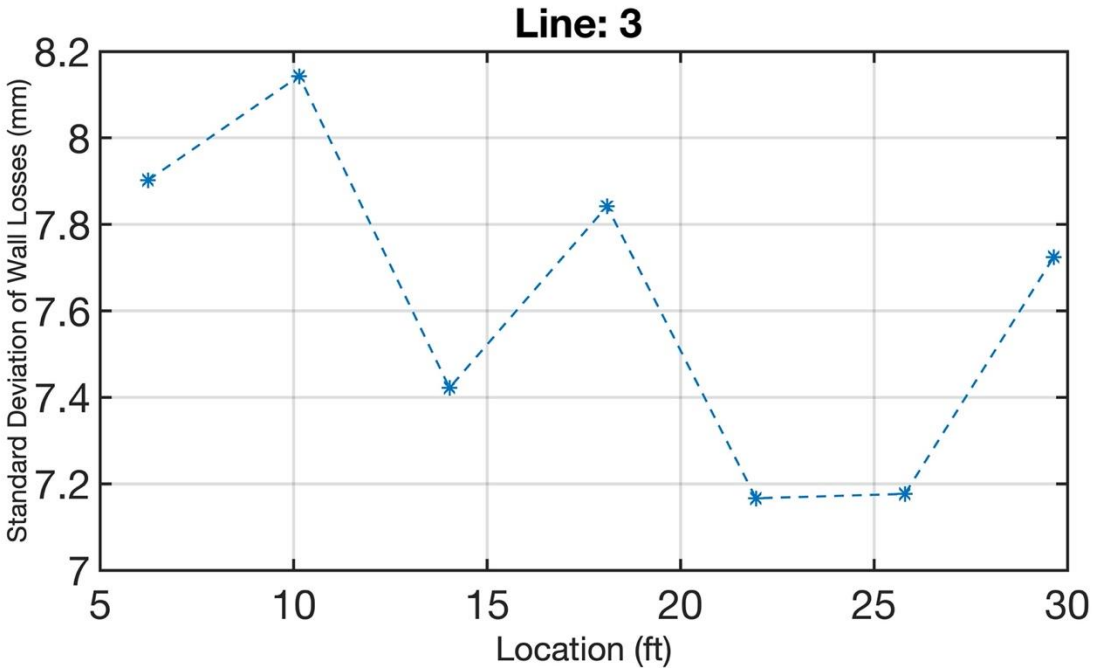

Figure 33. Comparing Half Normal standard deviation of losses for line 3.

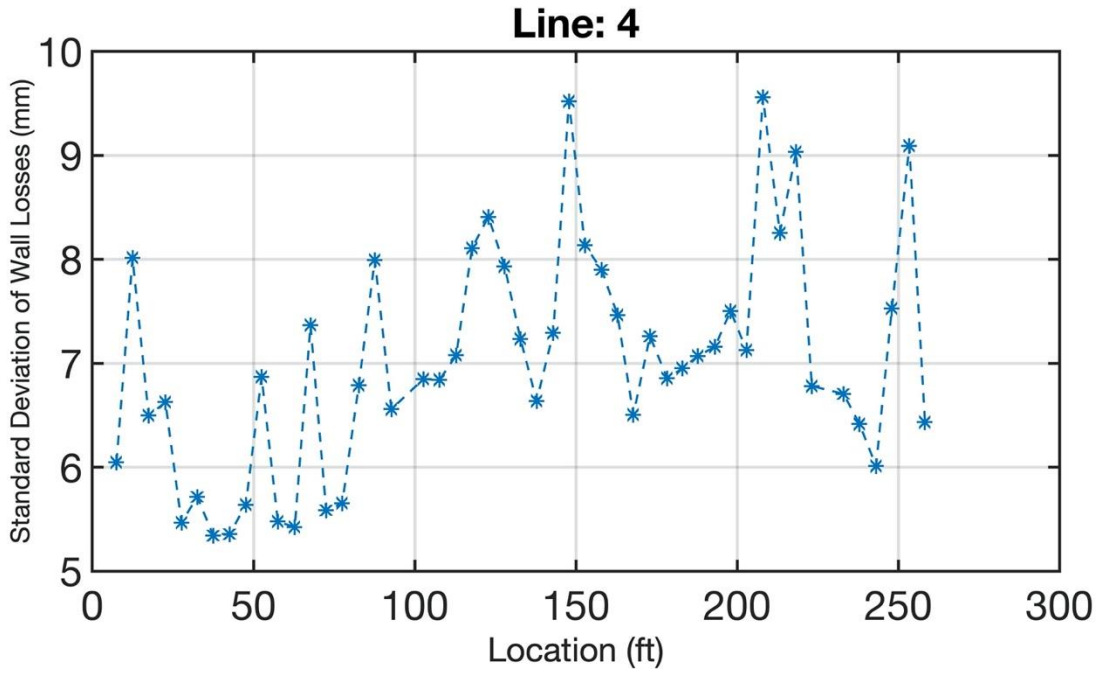

Figure 34. Comparing Half Normal standard deviation of losses for line 4.

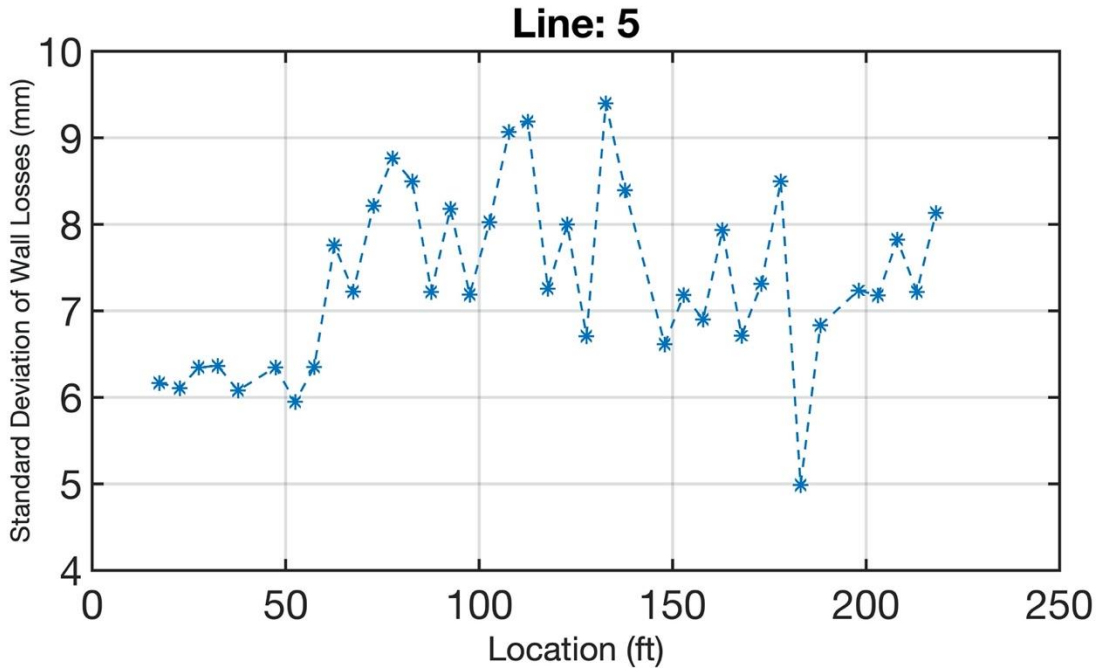

Figure 35. Comparing Half Normal standard deviation of losses for line 5.

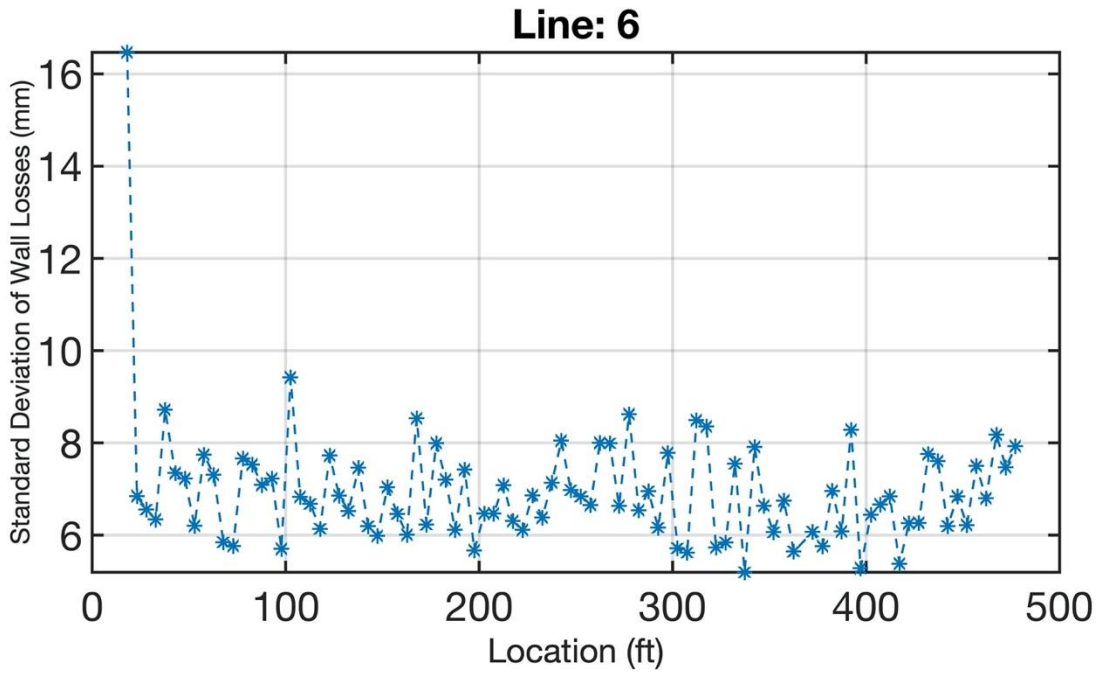

Figure 36. Comparing Half Normal standard deviation of losses for line 6.

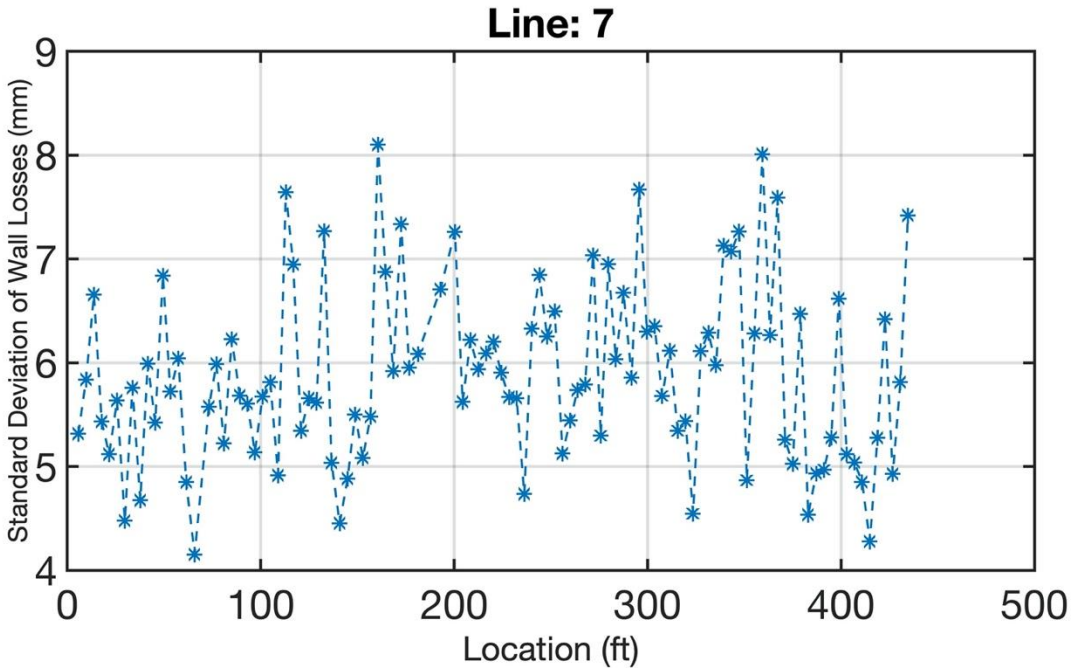

Figure 37. Comparing Half Normal standard deviation of losses for line 7.

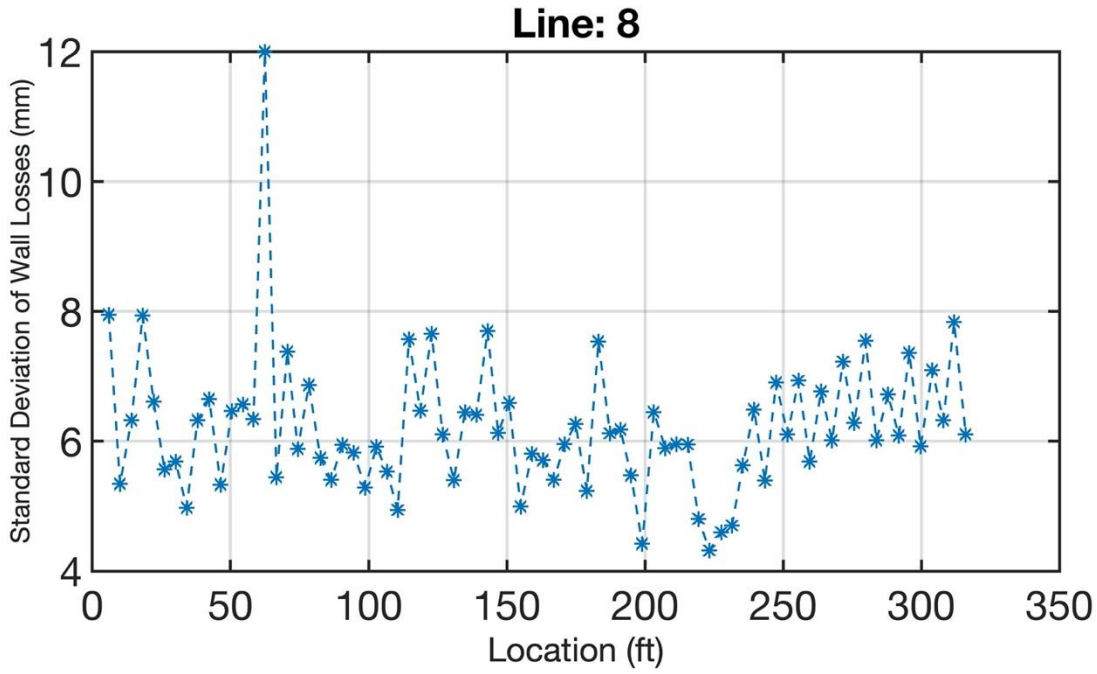

Figure 38. Comparing Half Normal standard deviation of losses for line 8.

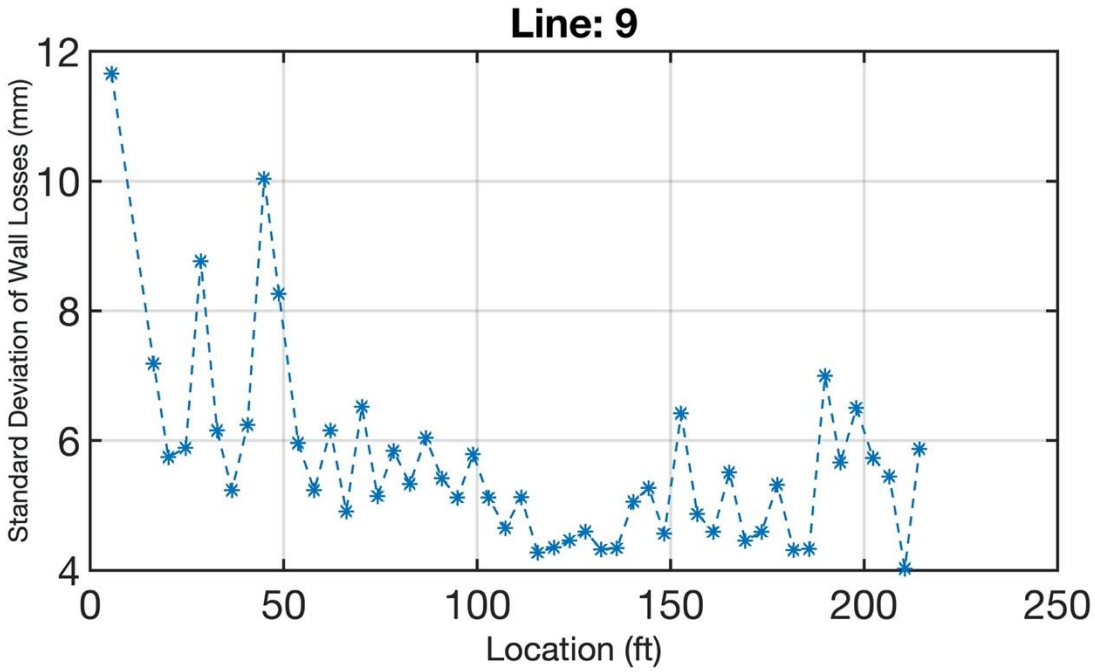

Figure 39. Comparing Half Normal standard deviation of losses for line 9.

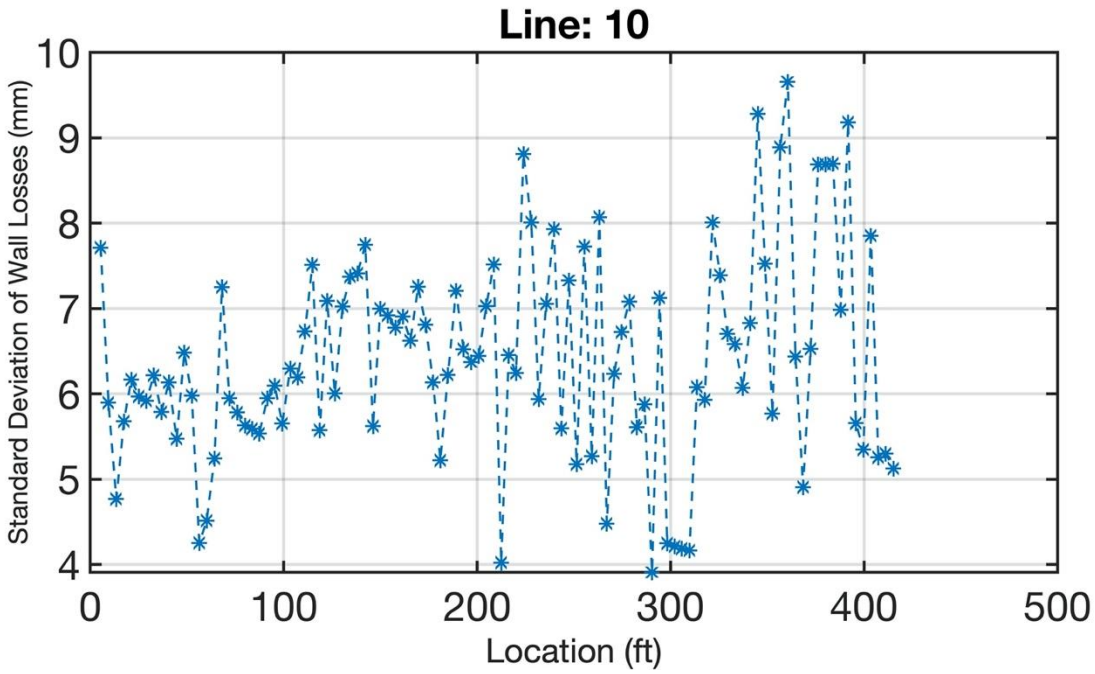

Figure 40. Comparing Half Normal standard deviation of losses for line 10.

Comparison of Figures 21-30 and Figures 31-40 certifies that the standard deviation of the Half-Normal distribution is following the same patterns as life expectancy method. This is of course intuitive since more loss leads to less service life. Therefore, this simplified method can be used

for determining which pipe requires more frequent inspection based on the peaks of the standard deviation plots

5.3. Results along the Length of each Pipeline (M-M)

The proposed automated framework is also capable of showing the results for each 1-inch rings along the length of each pipeline (Figures 41-50).

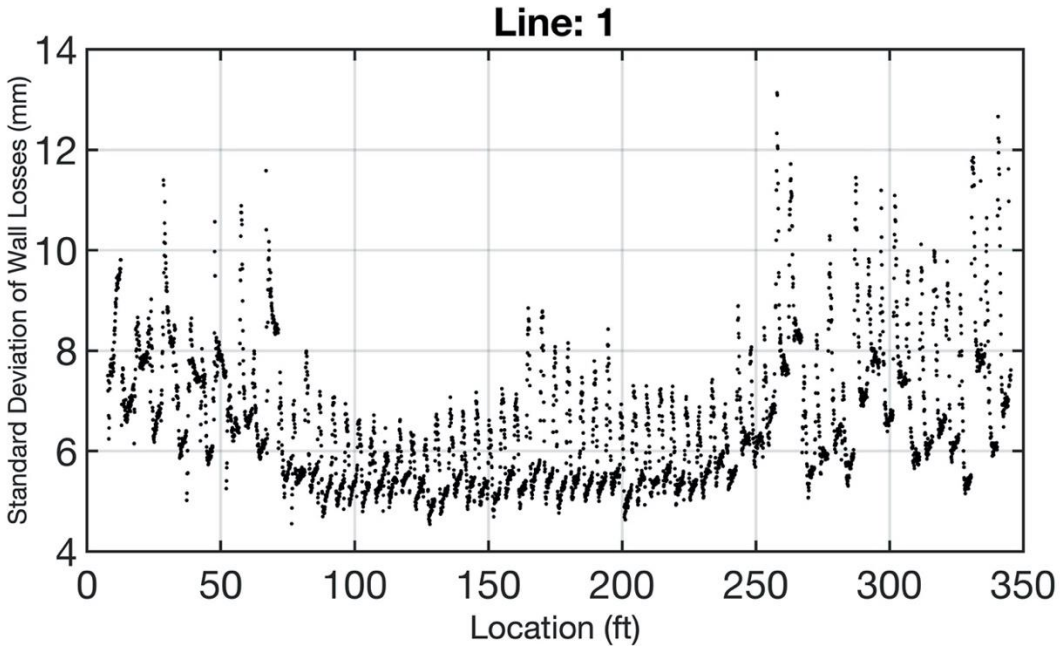

Figure 41. Standard deviation of losses along the length of pipeline (1 inch increment) for line 1.

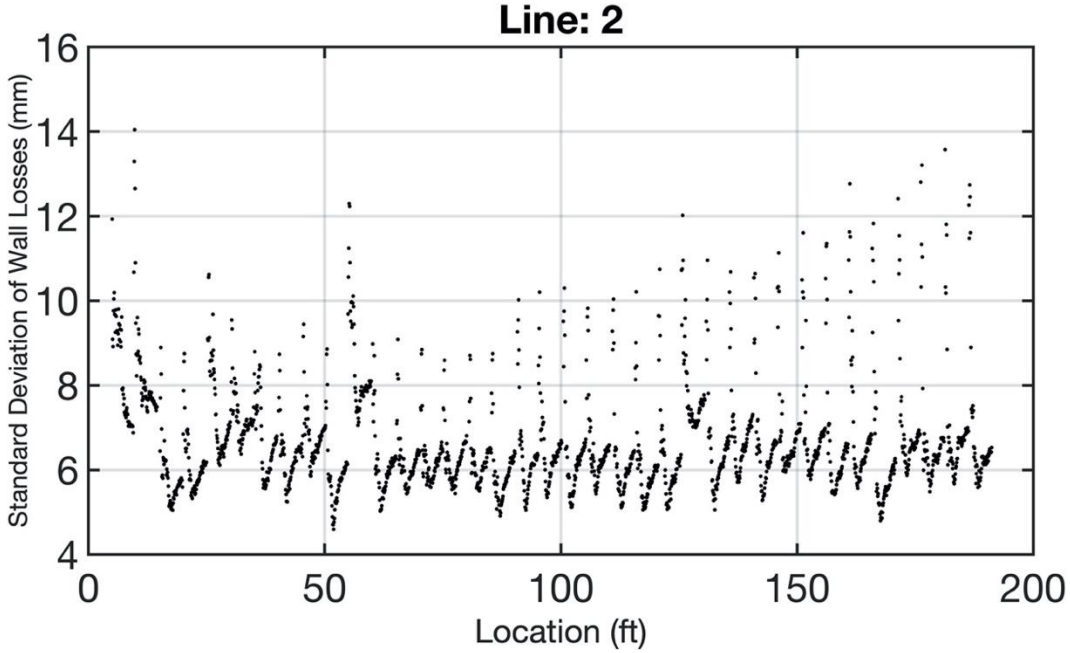

Figure 42.Standard deviation of losses along the length of pipeline (1 inch increment) for line 2.

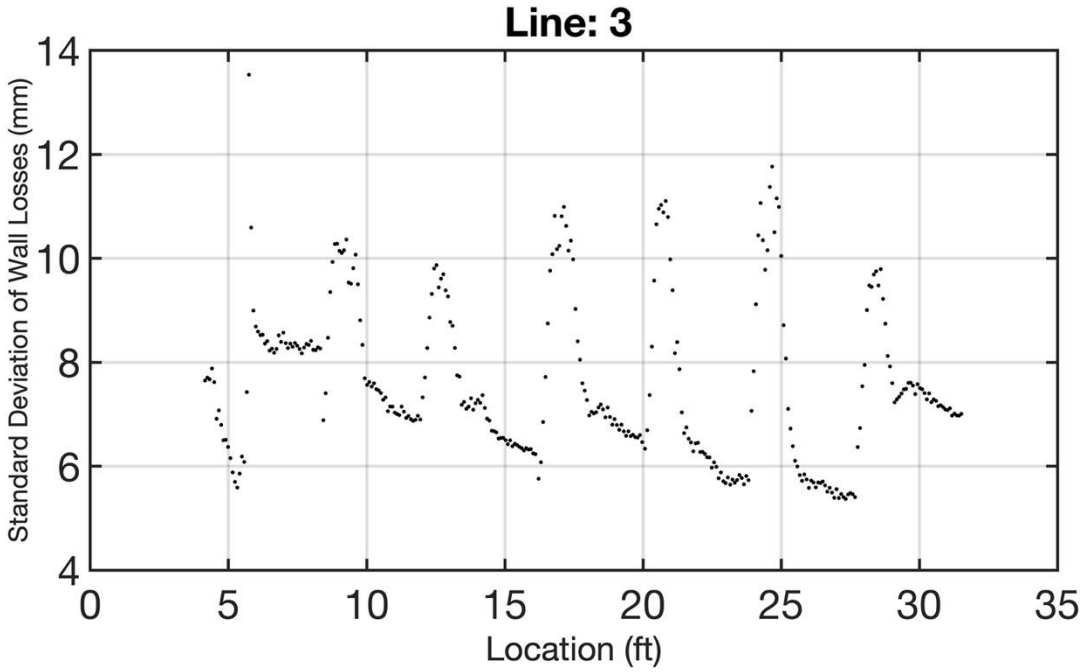

Figure 43.Standard deviation of losses along the length of pipeline (1 inch increment) for line 3.

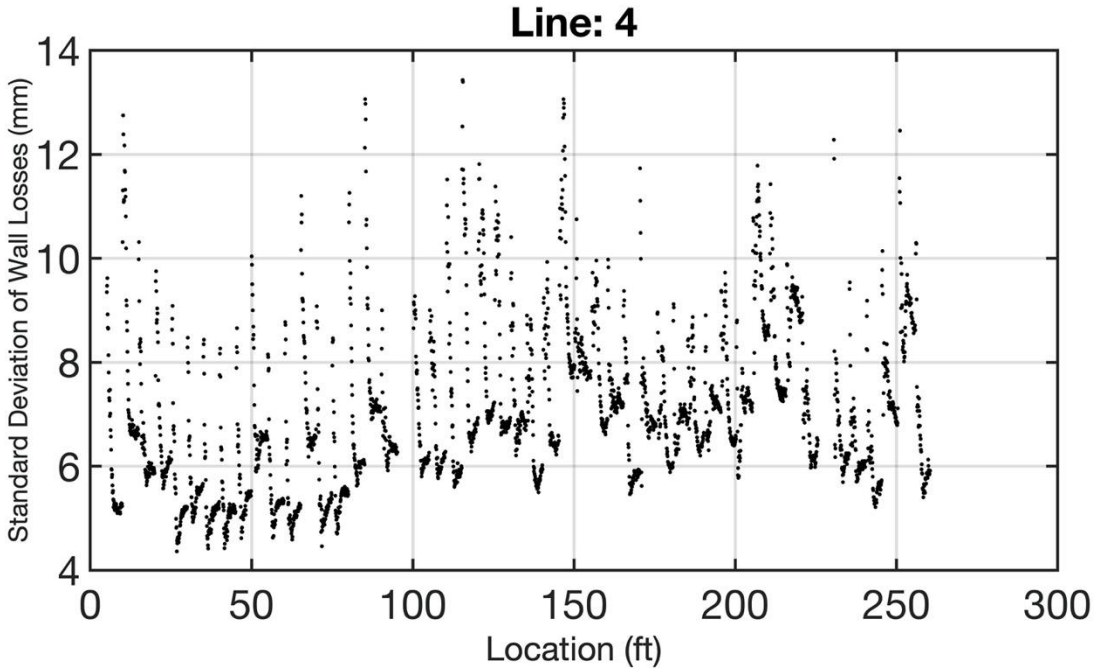

Figure 44. Standard deviation of losses along the length of pipeline (1 inch increment) for line 4.

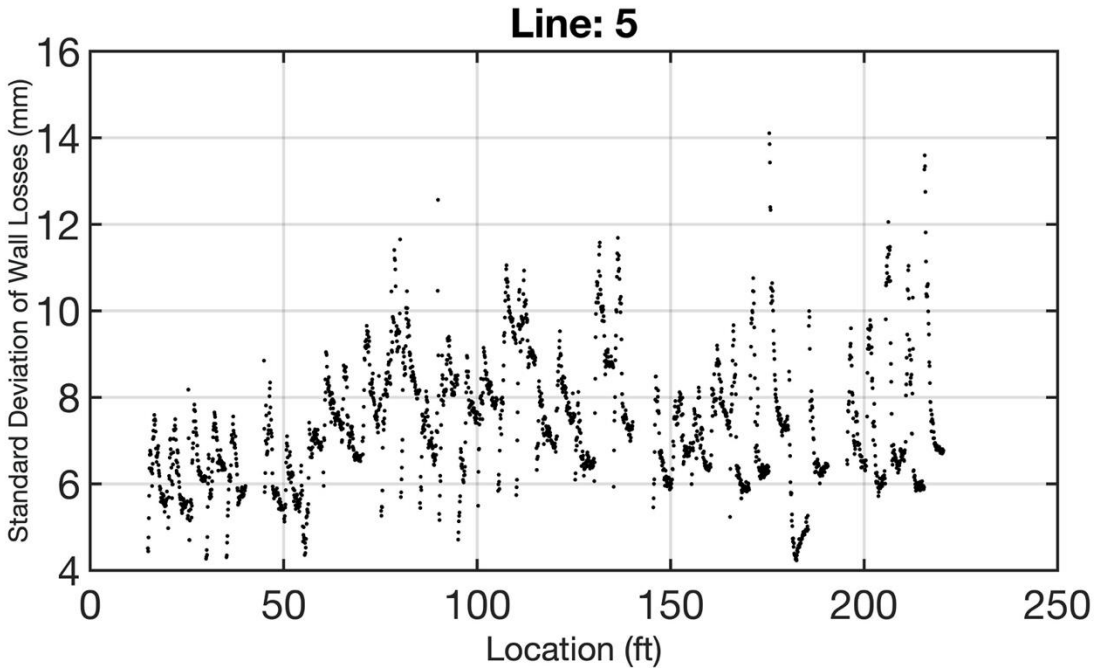

Figure 45. Standard deviation of losses along the length of pipeline (1 inch increment) for line 5.

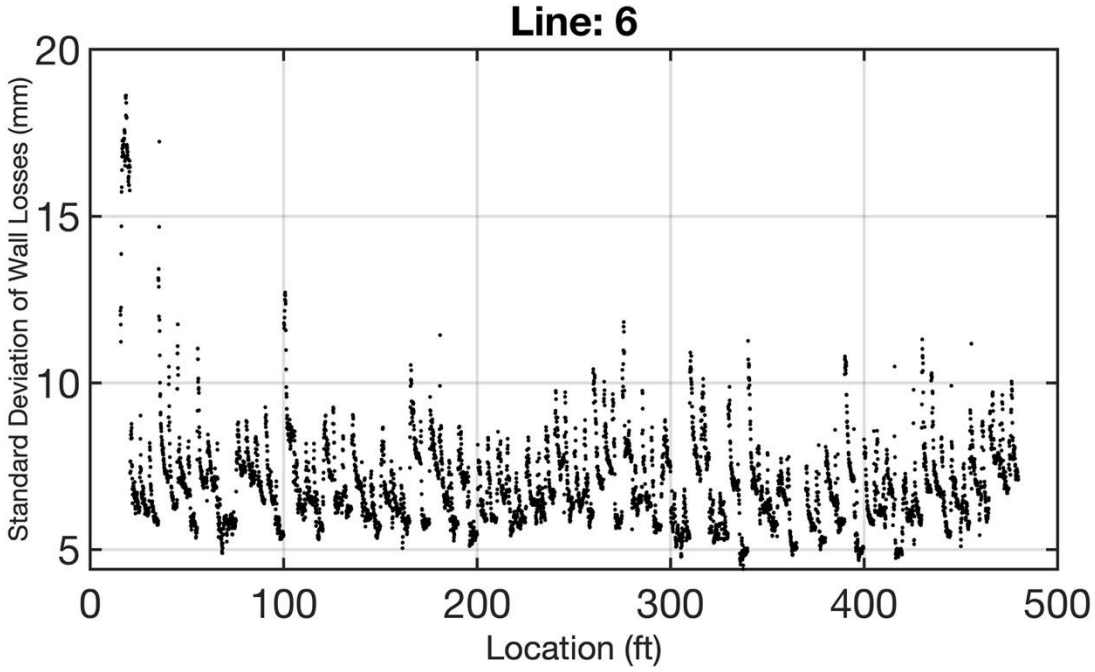

Figure 46. Standard deviation of losses along the length of pipeline (1 inch increment) for line 6.

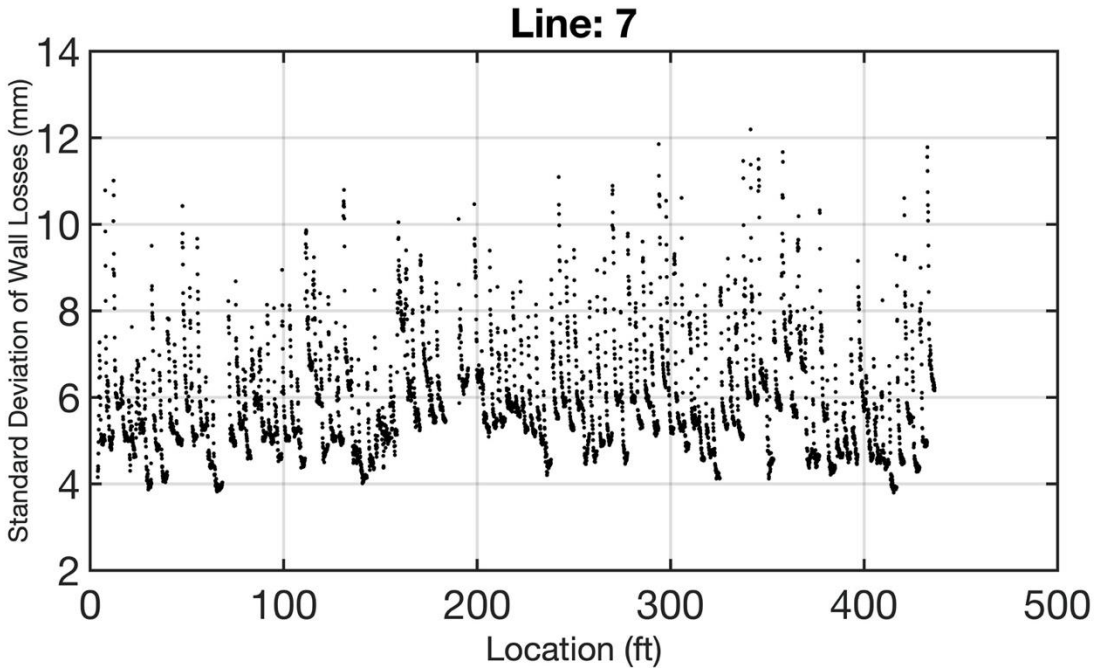

Figure 47. Standard deviation of losses along the length of pipeline (1 inch increment) for line 7.

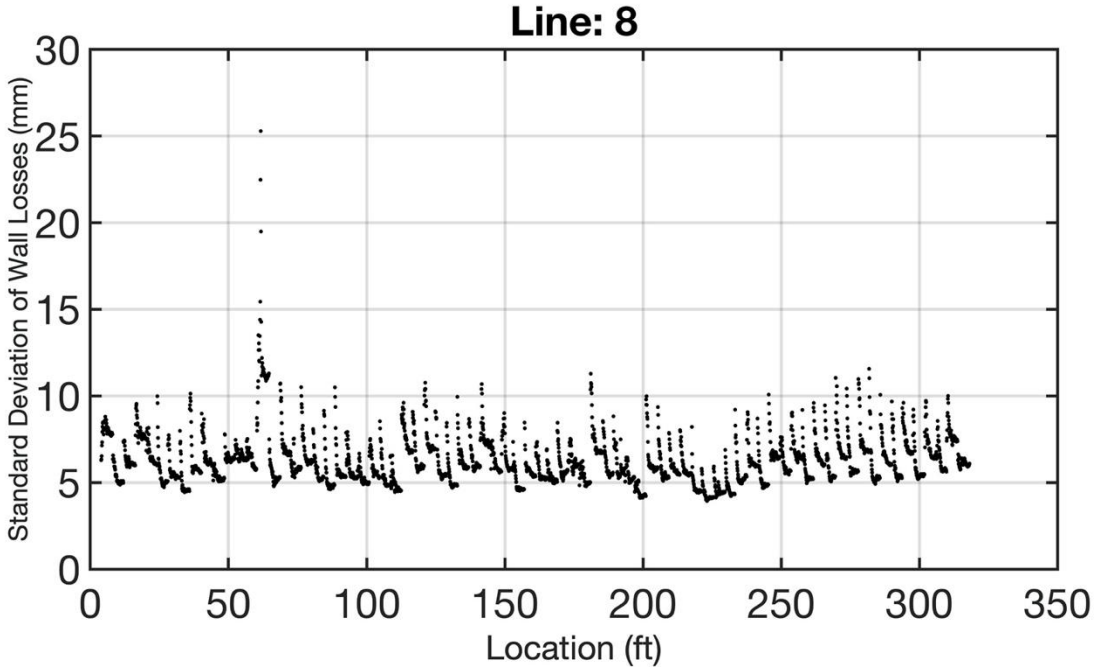

Figure 48. Standard deviation of losses along the length of pipeline (1 inch increment) for line 8.

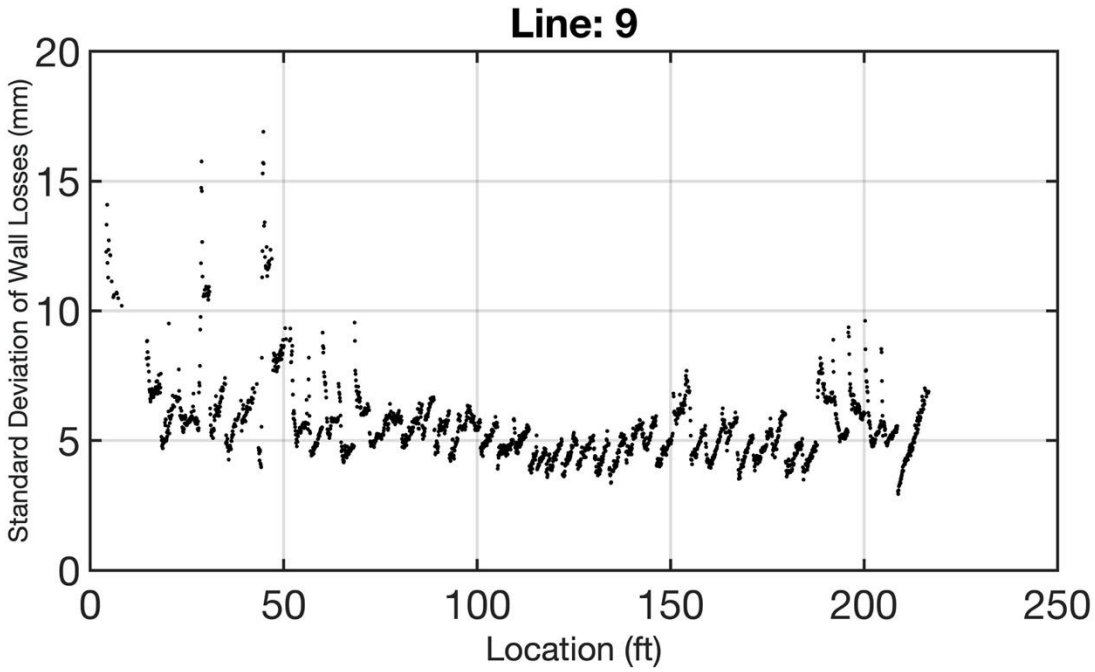

Figure 49. Standard deviation of losses along the length of pipeline (1 inch increment) for line 9.

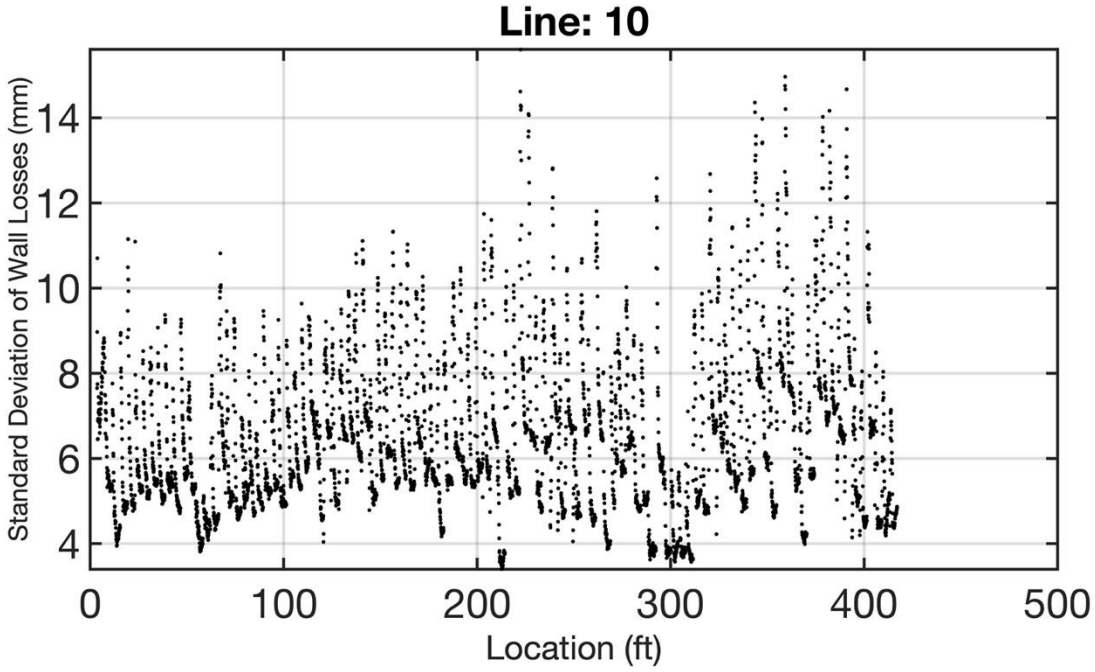

Figure 50. Standard deviation of losses along the length of pipeline (1 inch increment) for line 10.

5.4. Screenshots from CCTVs and Finding the Critical Locations/ Sections

The results from the proposed frameworks shows the location of each peak along the length of the inspected sewer pipes (which represents the higher losses). For the sake of brevity, screenshots of each critical 5-ft section are shown in Appendix A. The results are summarized in Table 2.

It should be noted that "Date of Expected Service" from Table 2, is calculated as follows: 2016 (i.e., inspection year) + Life expectancy using (Method 1 Section 4.4.5.1; Half Normal distribution).

Table 2. Verification using the critical locations of the selected lines (M-M)

Line #	Critical Section #	Critical Section Location (ft)	Average Loss (mm)	End Date for the Expected Servicability	Reference Figure (Appendix A)
1	13	69.4	8.7	2057	Figure 52.a
1	53	264.6	9	2056	Figure 52.b
1	67	333	8.8	2057	Figure 52.c
2	2	12	8.3	2059	Figure 53.a
2	11	57.4	8.6	2059	Figure 53.b
2	25	128	7.8	2062	Figure 53.c
4	4	19.2	7.61	2062	Figure 54
5	1	6.2	7.9	2059	Figure 55
6	28	147.9	9.5	2054	Figure 56. a
6	40	208	9.6	2055	Figure 56. b
6	48	253,4	9.1	2056	Figure 56. c
7	12	77.6	8.8	2057	Figure 57.a
7	19	112.6	9.2	2055	Figure 57.b
7	23	132.7	9.4	2054	Figure 57.c
8	18	102.5	9.4	2055	Figure 58
9	15	62.45	12	2044	Figure 59
10	4	17.8	10.65	2050	Figure 60.a
10	54	214.9	8.6	2057	Figure 60.b
10	60	238.1	8.9	2055	Figure 60.c

The critical location needs more in-depth inspection. Depending on the discretion of the municipalities and decision makers, the critical locations could be repaired, lined or replaced.

5.5. Recommendation for Future Work

Some of the pipelines in this project were rehabilitated (probably CIPP Liner). Figure 51 shows the CIPP liner on one of the selected pipelines. Unfortunately, there is not enough data and information available for evaluating the effect of rehabilitation on the pipelines and on increasing the life expectancy of the pipes.

Figure 51. CIPP liner inside the selected pipelines

To calculate the remaining life of RC pipelines more accurately, many parameters need to be considered such as:

a) Environmental factors of pipelines such as humidity, temperature, etc.

b) Mechanical properties of pipelines such as pipe diameter, initial ovality etc.

c) Sewer material such as content of corrosive materials (sulfide and chloride content)

In addition, the loss of wall thickness is only a serviceability performance index and there are ultimate limit state indicators that affect the reliability of RCPs as well. In addition, from an asset management point of view, a risk assessment methodology for RCPs subjected to both environmental and external load effects, including both the probability and the consequences of exceedance of a performance criteria is more efficient and accurate.

6. CONCLUSIONS

In current work, an automated data driven framework with minimal user interference is developed that uses LiDAR data from sewer inspections to obtain necessary information for estimation of pipe-wall thickness loss in sanitary sewer lines. The LiDAR point cloud of data, collected for each 5-ft. length of a pipeline (M-M), contains noises such as water level points and pipeline defects (e.g., root intrusion). After filtering and alignment of data cloud, each 5-ft section of the pipeline is divided into 60 rings, each having a length of 1-in. This allows to determine the wall thickness loss for each ring with greater accuracy. Once the pipe wall thickness loss is estimated using the filtered LiDAR data, corrosion rate is calculated by dividing the wall thickness loss amount to the age of the pipeline. Furthermore, a best distribution is fitted to wall thickness loss data. The goodness of fit is calculated by comparing R^2 values from least squares (LS) for QQ-plots of 11 different distribution. Finally, reliability is calculated considering serviceability limit state that defines failure as the complete loss of 1-in concrete cover. Considering this limit state and a prescribed probability of exceedance threshold, a reliability-based prediction of the remaining service life is determined for 1000 linear foot of large diameter RC sewer lines inspected by Redzone Robotics and CSER/SPI at University of Texas at Arlington with diameters of 54 and 60 inches. The result of the proposed approach is consistent, and reasonable with minimum user interference. The anticipated results can assist decision makers in prioritizing limited repair funding by providing a comprehensive, network-level, quantitative performance assessment of selected RC sanitary pipelines using the proposed automated framework.

More specifically, according to the obtained results the following conclusions can be drawn:

- Among the 11 considered PDFs for distribution of wall erosion, “Method 1” (method of probability of exceedance; section 4.4.5.1), shows more consistency and depicts more rational life expectancy comparing to “Method 2” (method of X-intercept section 4.4.5.2).
- By comparing life expectancy calculated by two different distributions, it is proven that Half Normal distribution is a safe alternative for well-known Weibull distribution to model the erosion rate.
- The automated framework performs consistently in term of calculating the life expectancy of RC pipelines.

REFERENCES

1. Shook, E.B.L. Corrosion Control in Concrete Pipe and Manholes. in International Conference on Water Environment federation. CSTI001, Orlando, Florida, 1998.

2. ASCE, *A Comprehensive Assessment of America's Infrastructure*. [Online] Available: https://infrastructurereportcard.org/wp-content/uploads/2020/12/National_IRC_2021-report.pdf.

Accessed January, 2022.

3. Stanić N., M. Lepot, M. Catieu, J. Langeveld, and H.L.R. Clemens. A technology for sewer pipe inspection (part.1) Design, calibration, corrections and potential application of a laser profiler. *Automation in Construction,* 2017. 75: 91–107.

4. Kaddoura, K. Automated Sewer Inspection Analysis and Condition Assessment. Masters thesis. Concordia University. 2015.

5. News. *West Side Road collapses week after massive sinkhole killed deputy*. 2016. [Online]. Available: https://www.mysanantonio.com/news/local/article/West-Side-road-collapses-week-after-massive-10793869.php. Accessed January, 2022

6. He, S., A. Koizumi. Damage Discrimination Analysis with Quantification Theory for Sewage Pipe System. *Journal of Pipeline Systems Engineering and Practice*, 2013. 4: 11-16.

7. Ribas-Silva, M. Study of biological degradation applied to concrete. in *Proceedings of Transactions of 13th International Conference on Structural Mechanics in Reactor Technology-SMiRT*, Porto Alegre, 1995.

8. C. Parker. Mechanics of Corrosion of Concrete Sewers by Hydrogen Sulfide. *Sewage and Industrial Wastes*, 1951. 23: 1477-1485.

9. Wells, T., R.E. Melchers, and P. Bond. Factors involved in the long-term corrosion of concrete sewers. in 49th Annual Conference of the Australasian Corrosion Association: Corrosion and Prevention, Coffs Harbour, Australia, 2009.

10. Pomeroy, R.D. *Process Design Manual for Sulfide Control in Sanitary Sewerage Systems*. U.S. Environmental Protection Agency, 1974.

11. Abuhishmeh, K. Service Life Prediction and Risk Analysis of Reinforced Concrete Gravity Flow Pipes using Reliability Theory. Masters Thesis. The Univesity of Texas at Arlington. 2019.

12. Moamaei, P. Remaining Service Life Estimation and Probabilistic Analysis of Reinforced Concrete Sewer Pipeline Systems. Masters Thesis. The Univesity of Texas at Arlington. 2019.

13. EPA. *Collection Systems O&M Fact Sheet Sewer Cleaning and Inspection*. Environmental Protection Agency, 1999.

14. Ékesm C., B. Neduczam and G.R. Henrich. GPR Goes Underground: Pipe Penetrating Radar. Presented at the North American Society for Trenchless Technology (NASTT) No-Dig Show, Washington, D.C., 2011.

15. Najafi, M. *Trenchless Technology Piping: Installation and Inspection*. The McGraw-Hill Companies, Inc, 2010.

16. Feng. Z., K.V. Horoshenkov, M.T. Bin Ali, and S. Tait. An acoustic method for condition classification in live sewer networks. in 18th World Conference on Nondestructive Testing(WCNDT), Durban, South Africa, 2012.

17. Duran, O., K. Althoefer, L.D. Seneviratne. Pipe inspection using a laserbased transducer and automated analysis techniques. *IEEE/ASME Transactions on Mechatronics*, 2003. 8: 401-409.

18. Al Asadi, M. Algorithm Development For Sewer Pipe System Condition Assessment Using Multi-Sensor (MSI) Technology. PhD dissertation. The University of Texas at Arlington. 2018.

19. Tuccillo, M.E., J. Jolley, K. Martel, G. Boyd. Report on Condition Assessment of Wastewater Collection Systems, Report EPA/600/R-10/101. United States Environmental Protection Agency, 2010.

20. Redzone. *Redzone Robotics, Multi-Sensor Inspection*. 2021. [Online]. Available: http://www.redzone.com/services/msi. Accessed August, 2021.

21. Papoulis, A. and S.U. Pillai. *Probability, Random Variables, and Stochastic Processes*. McGraw-Hill: Mathematics, 2002.

22. Altman, D. G. and J. M. Bland. Measurement in medicine: the analysis of method comparison studies. *Journal of the Royal Statistical Society. Series D (The Statistician)*, 1983. 32: 307-317.

23. ASTM C76-20. *Standard Specification for Reinforced Concrete Culvert, Storm Drain, and Sewer Pipe*. 2020.

24. Matt, J. *3D Rotation about Shifted Axis*. [Online]. Available: https://www.mathworks.com/matlabcentral/fileexchange/30864-3d-rotation-about-shifted-axis. Accessed January, 2022.

25. Sumith, Y. Fast Circle fitting using Landau Method. [Online]. Available: https://www.mathworks.com/matlabcentral/fileexchange/44219-fast-circle-fitting-using-landau-method. Accessed January, 2022.

APPENDIX A: CCTV IMAGES OF THE INSPECTED SEWER LINES

In this part, the screenshots of the critical 5-ft section are provided from the CCTVs.

A.1. Critical Sections of Line 1

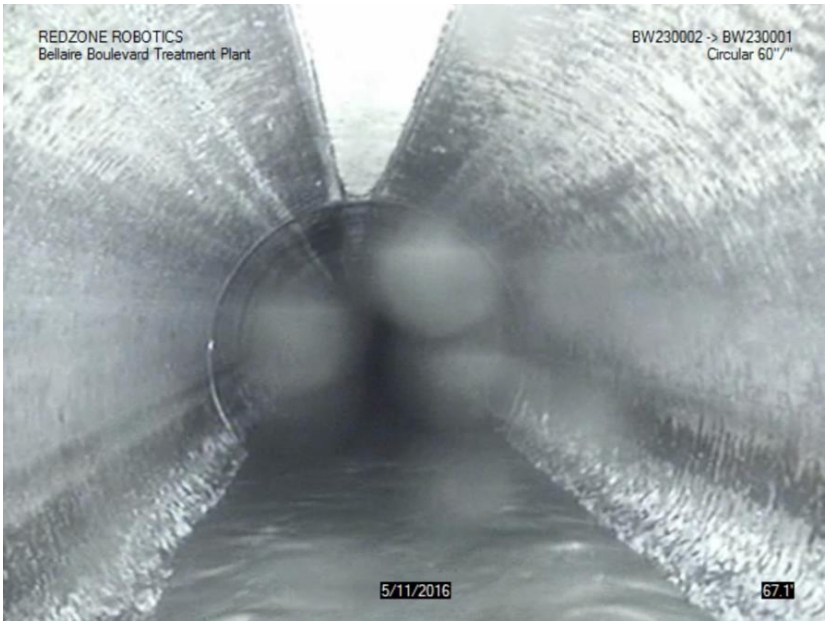

(a)

(b)

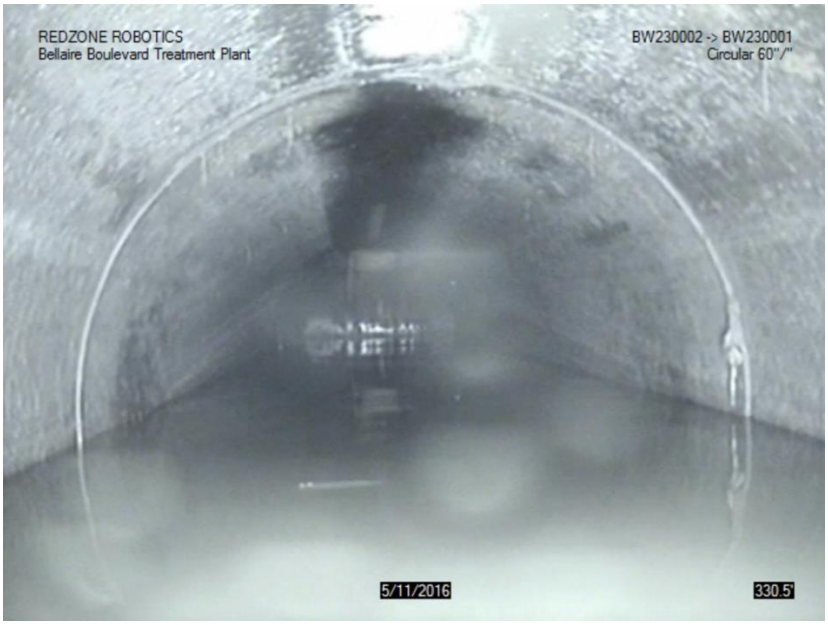

(c)

Figure A1. Screenshots from Critical Sections of Line 1

A.2. Critical Sections of Line 2

(a)

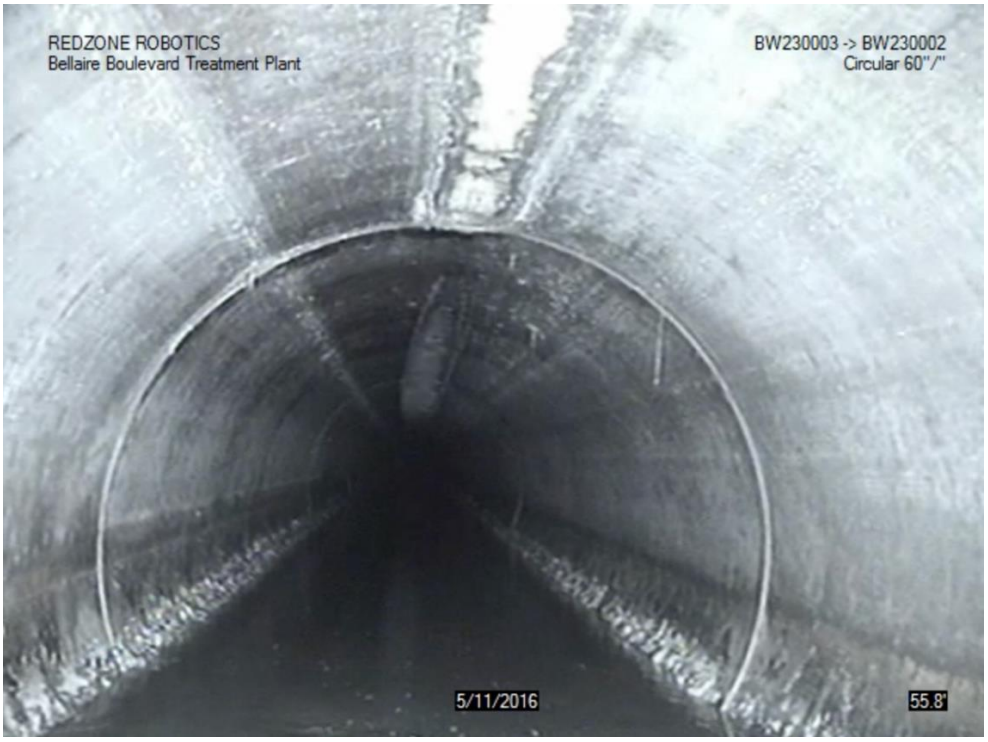

(b)

(c)

Figure A2. Screenshots from Critical Sections Line 2

A.4. Critical Sections of Line 4

Figure A3. Screenshots from Critical Sections Line 4

A.5. Critical Sections of Line 5

Figure A4. Screenshots from Critical Sections Line 5

A.6. Critical Sections of Line 6

(a)

(b)

(c)

Figure A5. Screenshots from Critical Sections Line 6

A.7. Critical Sections of Line 7

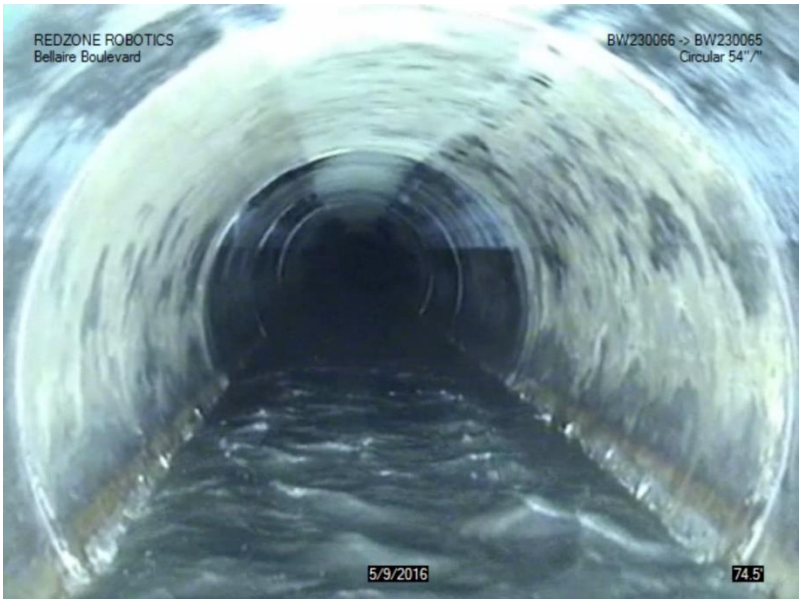

(a)

(b)

(c)

Figure A6. Screenshots from Critical Sections Line 7

A.8. Critical Sections of Line 8

Figure A7. Screenshots from Critical Sections Line 8

A.9. Critical Sections of Line 9

Figure A8. Screenshots from Critical Sections Line 9

A.10. Critical Sections of Line 10

(a)

(b)

(c)

Figure A9. Screenshots from Critical Sections Line 10

APPENDIX B: FITTING DIFFERENT PDFS TO THE MEAN WALL THICKNESS LOSSES OF THE INSPECTED SEWER LINES

The methodology in this research measures a goodness of fit by comparing R^2 values for fitted line to QQ-plots of each 1" rings. Fig.6 shows the results for the distribution fitting algorithm, while Table 2 summarizes the R^2 values

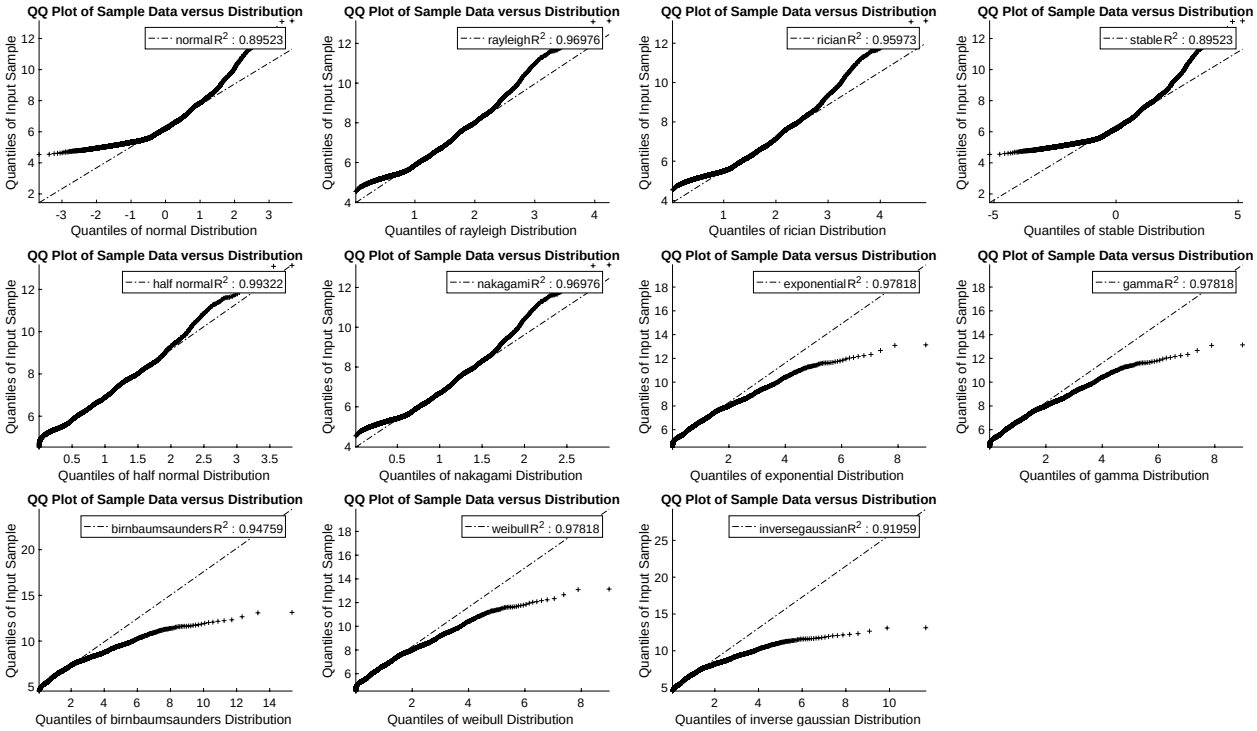

Line number: 1

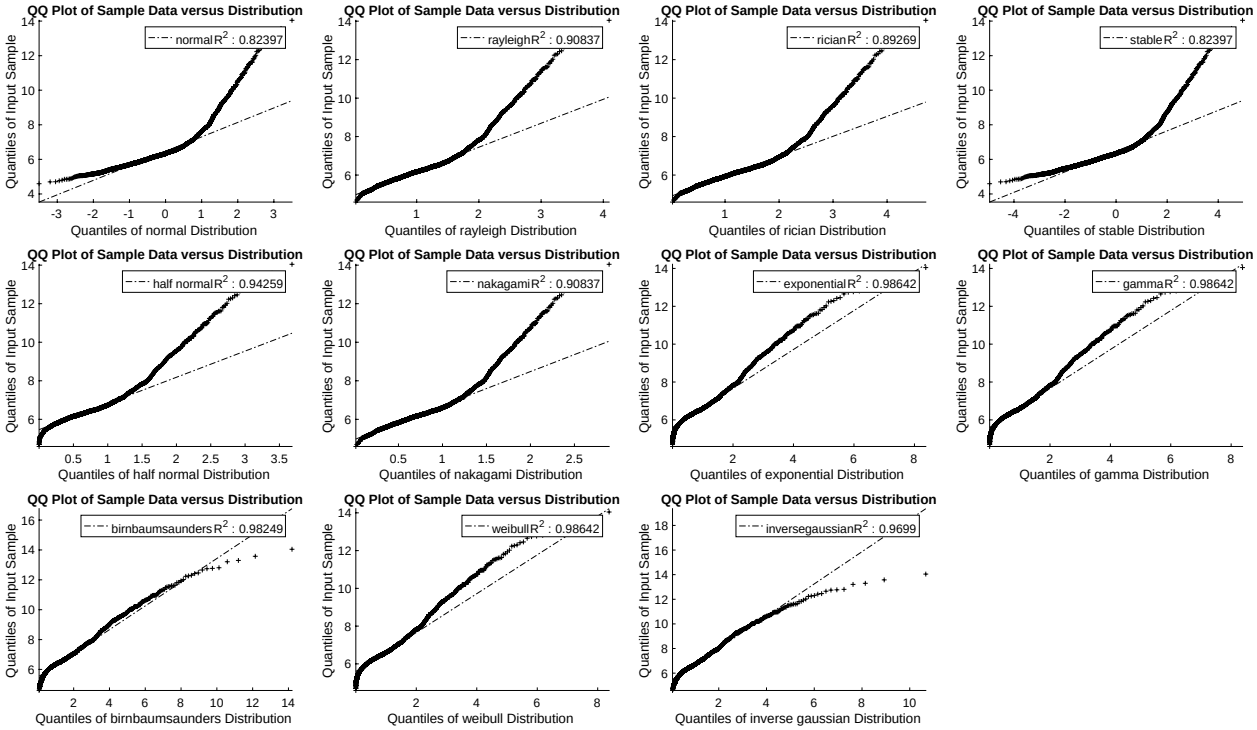

Line Number :2

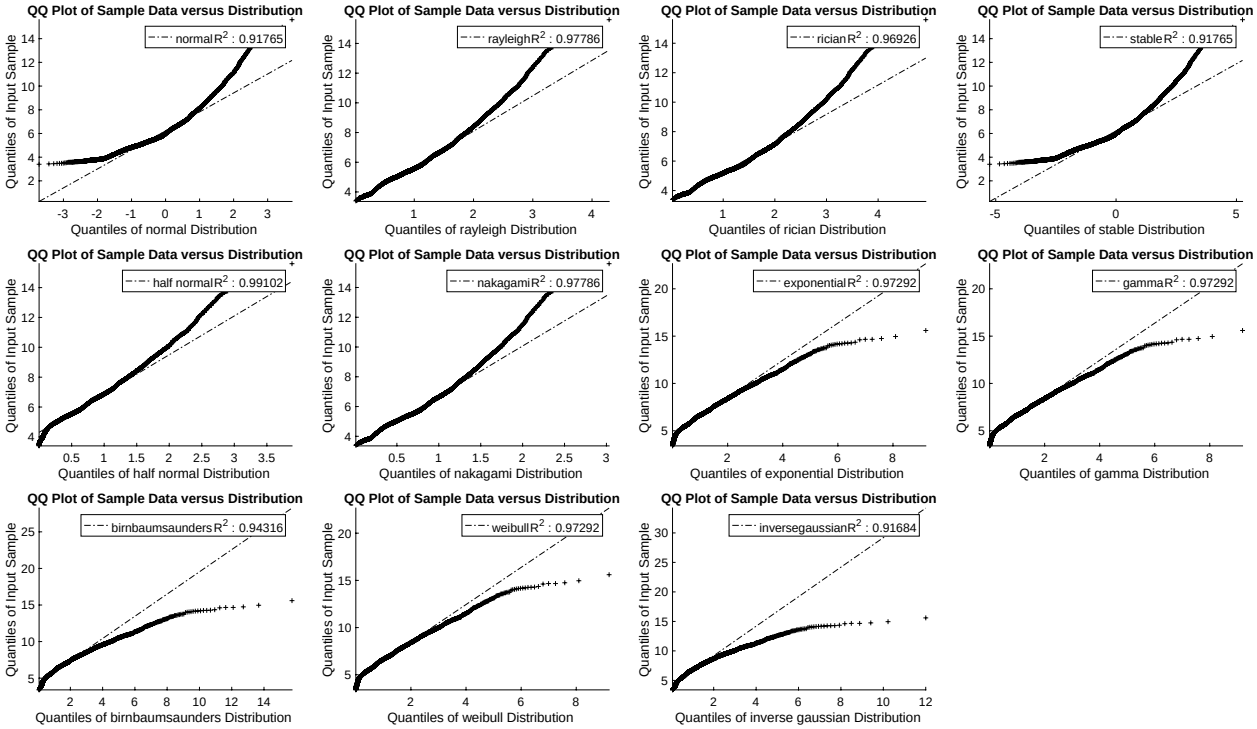

Line number: 3

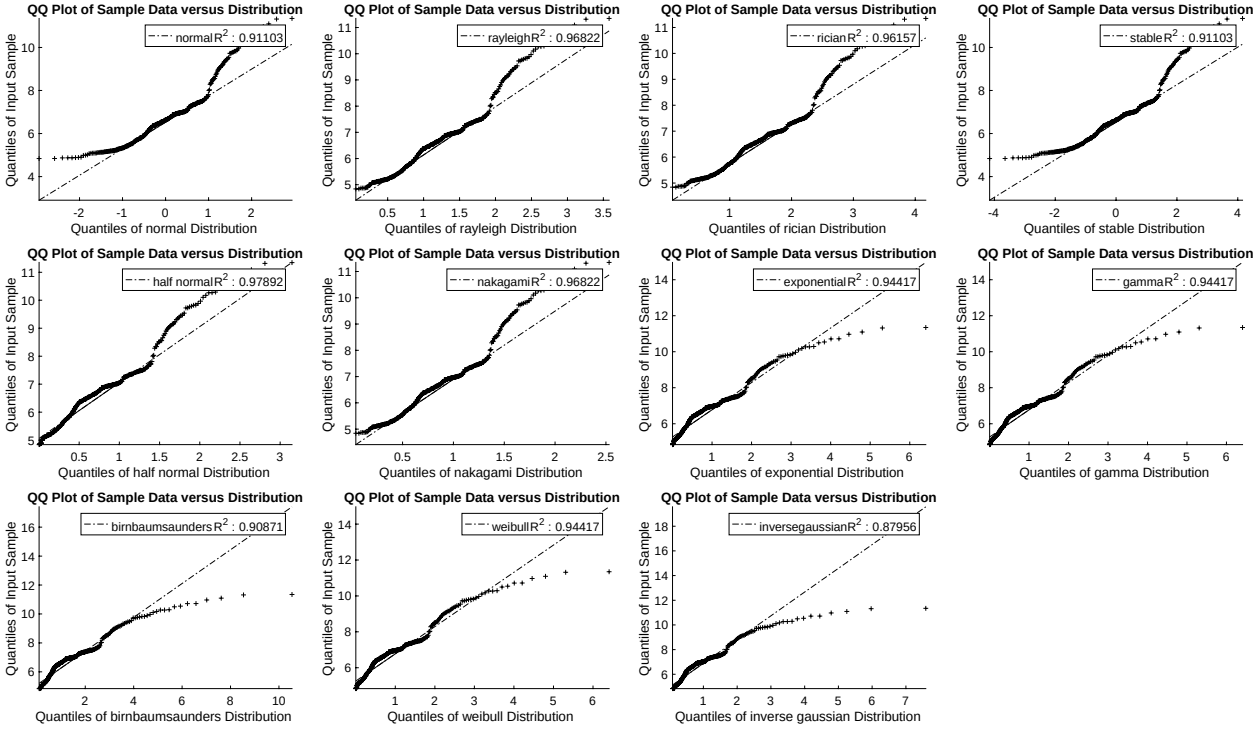

Line number: 4

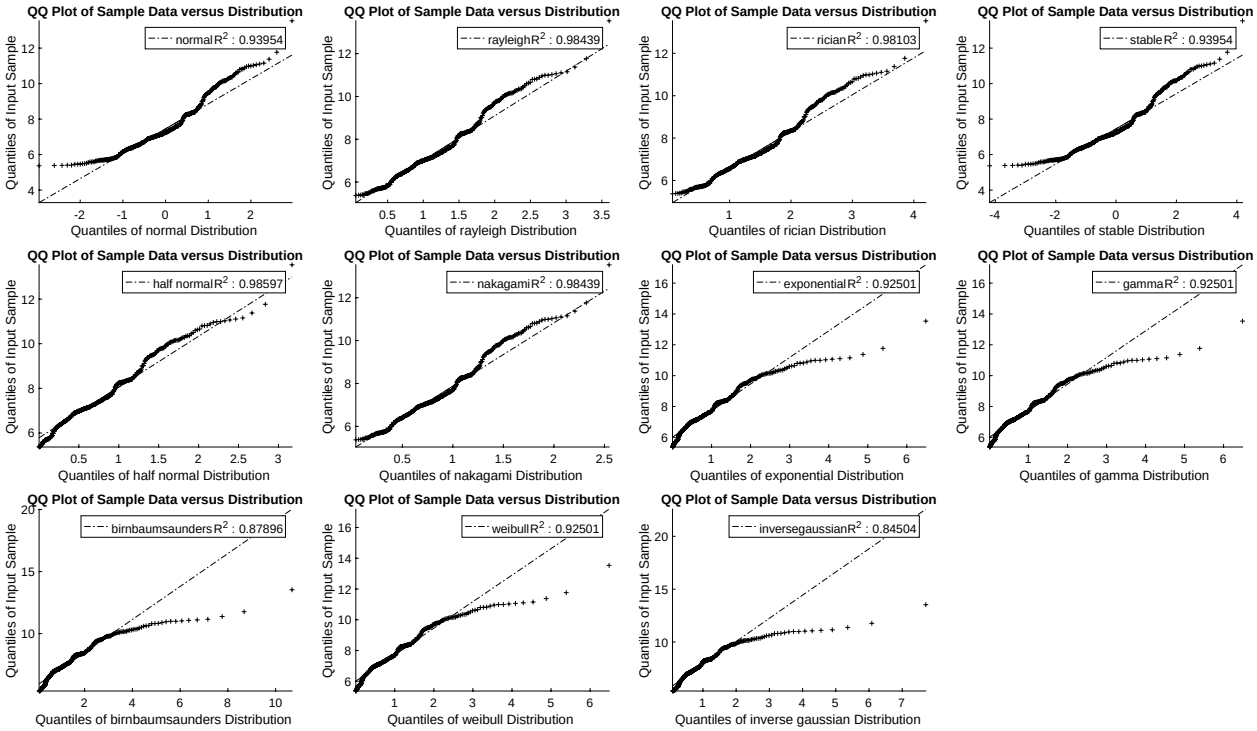

Line number: 5

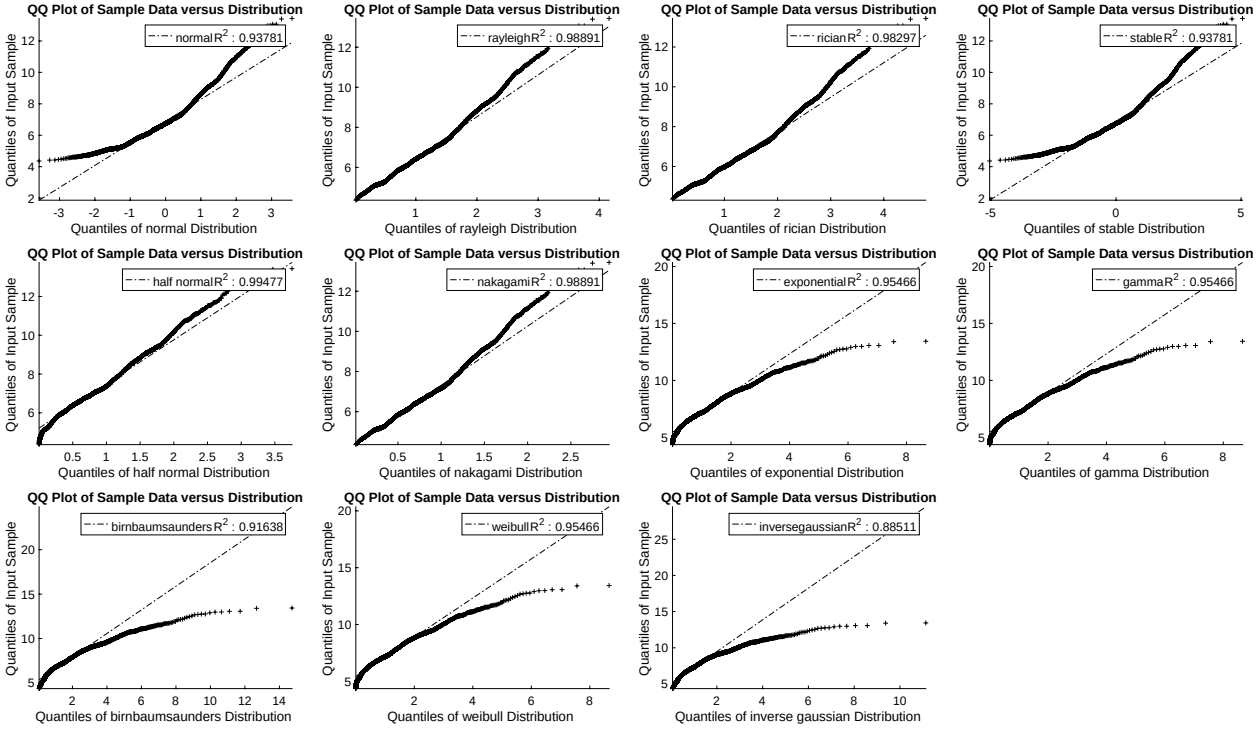

Line number: 6

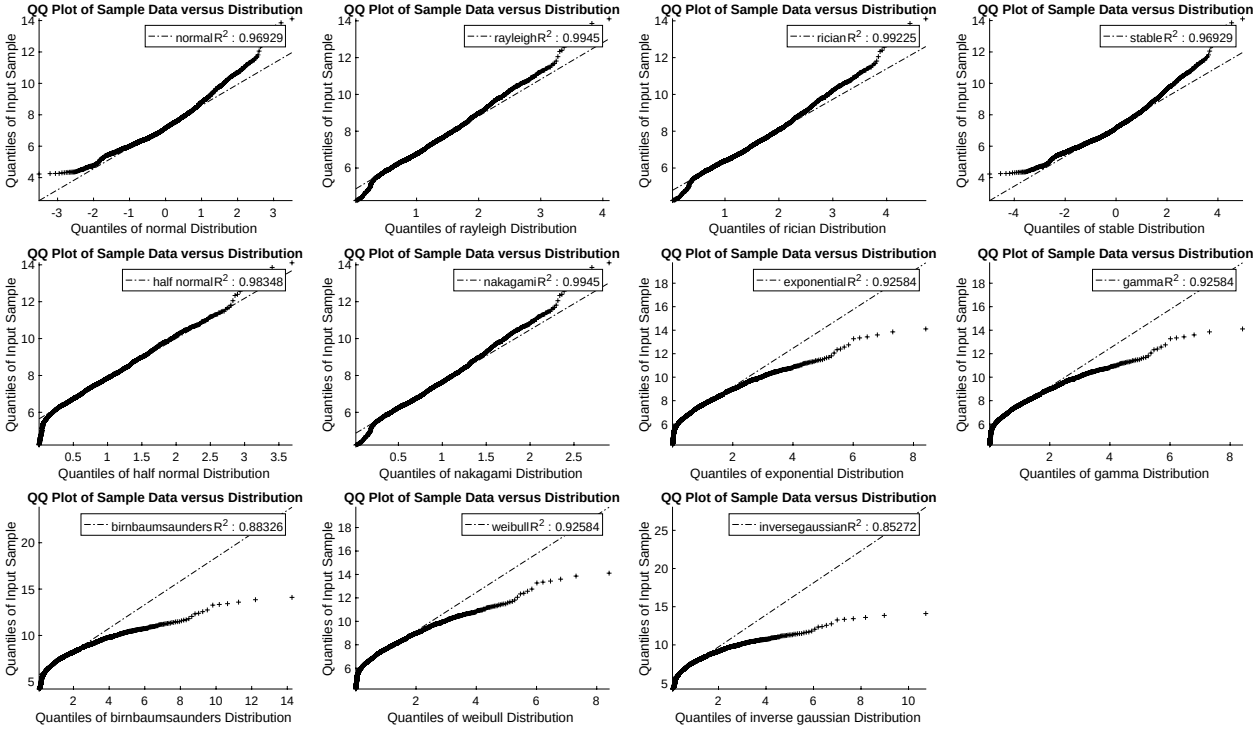

Line number: 7

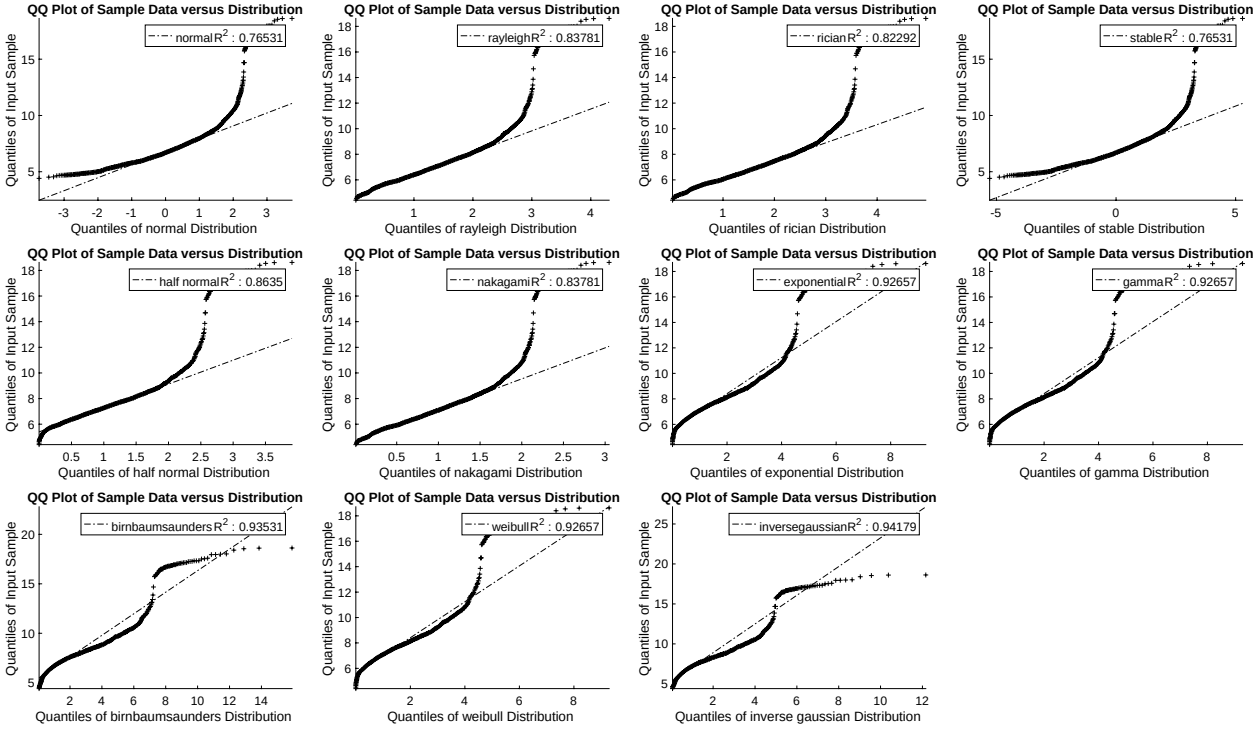

Line number: 8

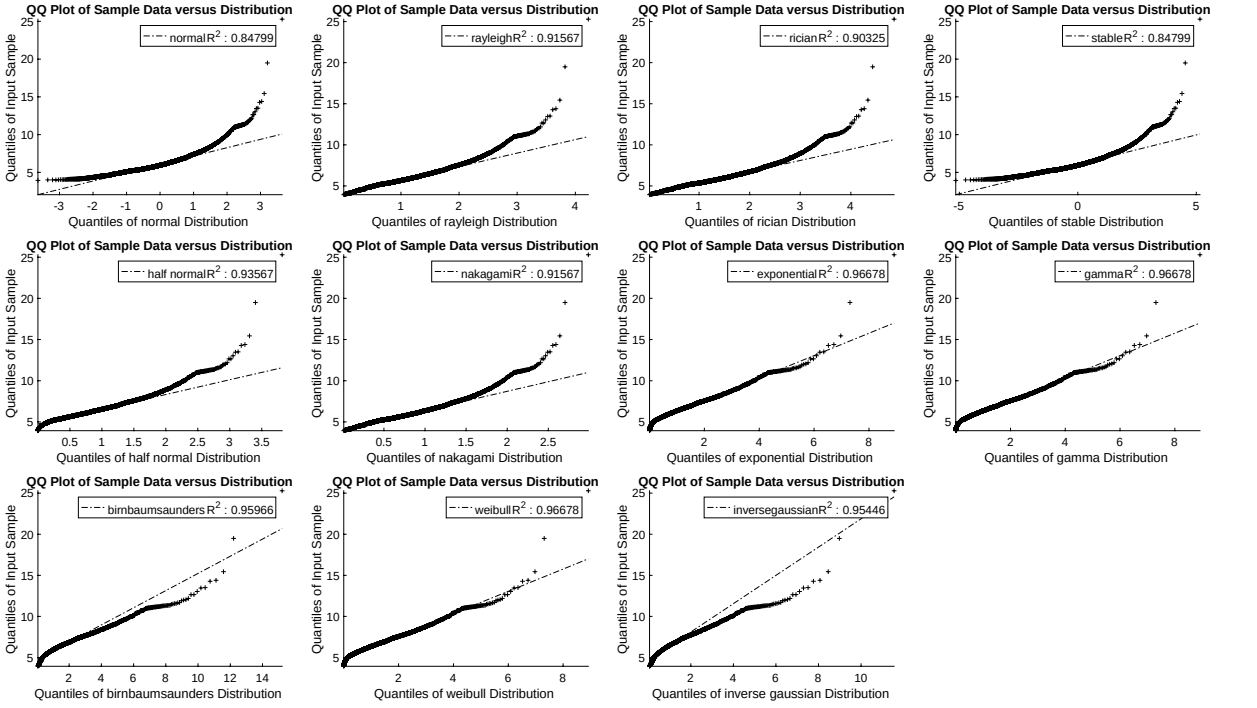

Line number: 9

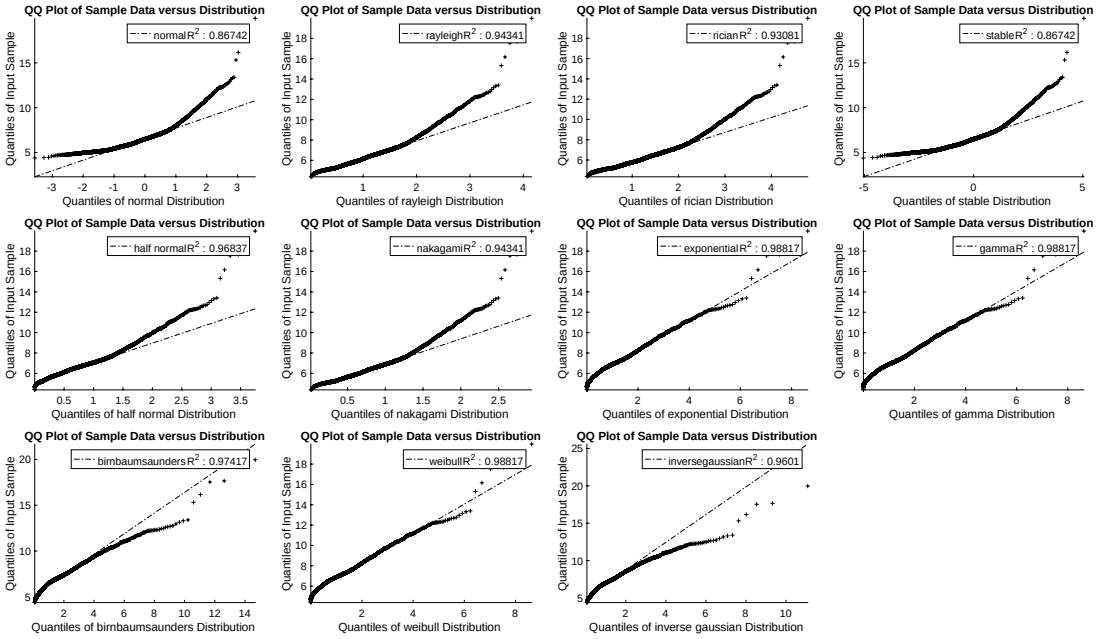

Line number: 10

Fig. B1. Results for fitting different distribution to the mean wall losses of all 1-in rings and their r^2 values

Table B1. R^2 values for different wall-thickness loss for four of the distribution for the mean wall losses of all 1-in rings of the selected pipelines.

Line Number	Half Normal	Weibull	Normal	Exponential
1	0.9932178	0.978184	0.895234	0.97818362
2	0.9425863	0.986417	0.823965	0.98641707
3	0.9910176	0.97292	0.917648	0.9729201
4	0.9789172	0.944173	0.944173	0.94417268
5	0.9859686	0.925013	0.925013	0.92501281
6	0.9947731	0.954658	0.954658	0.95465812
7	0.9834837	0.925838	0.925838	0.92583791
8	0.8634997	0.926568	0.926568	0.92656845
9	0.9356701	0.966783	0.966783	0.96678305
10	0.9683671	0.988174	0.988174	0.98817363